# DISTRIBUTION AND ABUNDANCE OF BEAKED WHALES AND OTHER DEEP DIVING CETACEANS IN EUROPEAN ATLANTIC WATERS

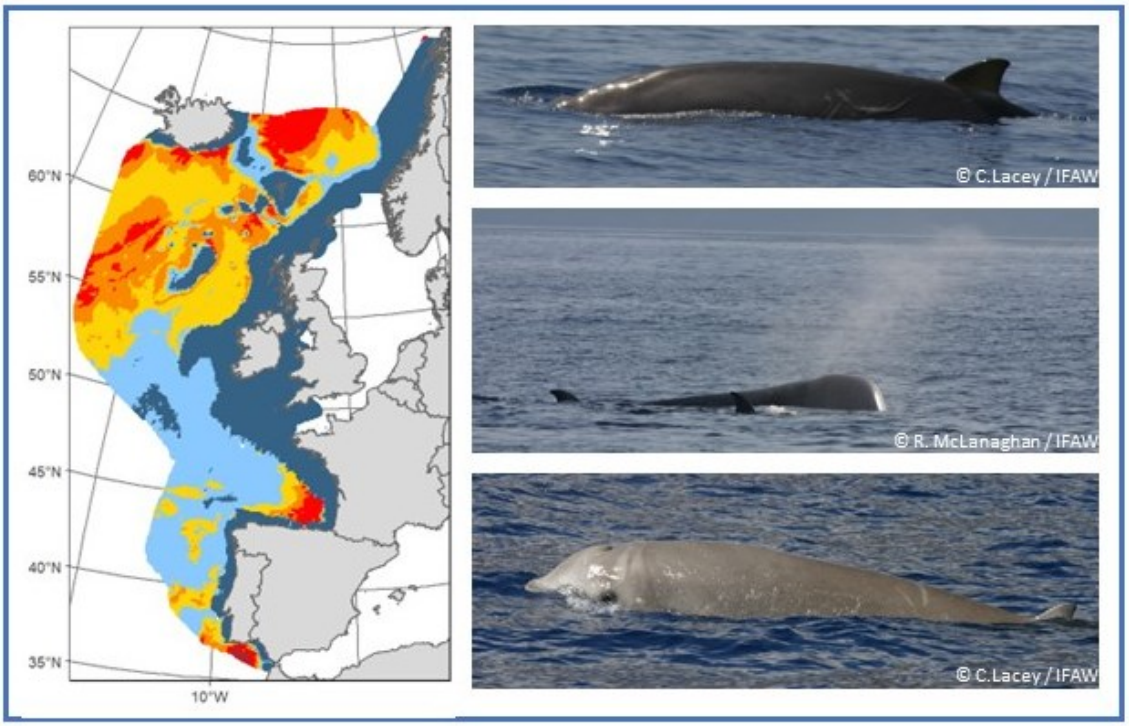


C Lacey & PS Hammond

November 2023

# DISTRIBUTION AND ABUNDANCE OF BEAKED WHALES AND OTHER DEEP-DIVING CETACEANS IN EUROPEAN ATLANTIC WATERS

C Lacey & PS Hammond
Sea Mammal Research Unit, Scottish Oceans Institute, University of St Andrews, St Andrews, UK

November 2023

## This report should be cited as:

Lacey, C. & Hammond, P.S. 2023. Distribution and abundance of beaked whales and other deep diving cetaceans in European Atlantic waters. Report to BEIS. 59pp.

## Acknowledgements

This work was funded through the UK Department for Business, Energy and Industrial Strategy's Offshore Energy Strategic Environmental Assessment programme. Data used in this report were from the SCANS series of surveys, the ObSERVE surveys in Irish waters, and the T-NASS/NASS in Faroese wates. SCANS-II 2005, CODA 2007, and SCANS-III 2016 data are curated at SMRU, University of St Andrews on behalf of the SCANS series of projects. Permission to use the ObSERVE data was granted by the Department of Communications, Climate Action and Environment and the National Parks and Wildlife Service, Department of Culture, Heritage and the Gaeltacht, Ireland (see also Rogan et al. 2018); processed data were made available by Ana Cañadas. Permission to use the Faroe Islands T-NASS 2007 and NASS 2015 data was received from Bjarni Mikkelsen, Faroese Museum of Natural History, Torshavn, Faroe Islands; processed data were made available by Nadya Ramirez.

# Contents

# 1 Introduction

Beaked whales (family Ziphiidae) are very difficult to study at sea. They inhabit an offshore environment, perform long dives of typically an hour or more and are usually only visible for short periods at the surface (e.g. Tyack et al. 2006, MacLeod 2017). A single surfacing lasts only a few seconds, with a whole surfacing series lasting only 2-3 minutes (Barlow 1999; Shearer et al. 2019) and producing little to no visible blows (Zimmer et al. 2008). Studies have estimated the probability of visual detection on a survey transect line to be 0.276 for Cuvier's beaked whale (*Ziphius cavirostris*) in sea conditions of Beaufort 2, dropping to 0.09 in Beaufort 5, which may be more representative of the conditions most frequently encountered offshore (Barlow et al. 1999).

Due to very similar morphology, some species of the genus *Mesoplodon* can also be difficult to identify to species level (Macleod et al. 2006), which may, in some cases, require a clear view of the position of the erupted teeth of the adult males (Pitman 2018). This is not feasible at distance, and it can be difficult to approach for a more detailed look with a large survey ship, notwithstanding that the individuals sighted may be female or juvenile, in which case the diagnostic teeth would not be present. Overall, small beaked whales can be amongst the most difficult cetacean species to detect and identify on survey (Barlow et al. 2006). This has contributed to a paucity of information on distribution of these species in the north-eastern Atlantic, with large scale shelf surveys rarely collecting enough detections to produce an estimate of density.

These species can be good candidates for passive acoustic monitoring (PAM). Deep diving odontocetes are known to echolocate routinely in association with foraging events. Whilst the ascent and parts of the descent phases of long dives are thought to be silent, during the foraging phases a variety of different echolocation clicks are made (e.g. Johnson et al. 2004; Zimmer et al. 2008; Aguilar de Soto et al. 2012). Beaked whale clicks are frequency modulated upsweep pulses, and they seem to be species specific, with unique temporal and spectral characteristics (Baumann-Pickering et al. 2013), allowing detections to be identified to species. By towing a hydrophone behind a survey vessel, it is possible to collect acoustic data which can augment or, indeed, supersede the data collected by visual observers alone (Stanistreet et al. 2017).

As well as beaked whales, two other deep diving cetacean species occur regularly in the north-eastern Atlantic, the long-finned pilot whale (*Globicephala melas*), and the sperm whale (*Physeter macrocephalus*). Whilst these species can be much easier to detect at the surface, due to having longer surfacing times, more visible blows, and being less cryptic (Jaquet et al. 2000; Watwood et al. 2006) sperm whales dives may still last an hour or more (Watkins et al. 1993), so they present limited availability at the surface to be detected by survey teams.

Long-finned pilot whales are a little different to the other deep diving species. Whilst they routinely dive to depths of up to 600m, tagging studies have revealed that long-finned pilot whales spend more than half of their time near the sea surface, within the top 7m (Baird et al. 2002; Heide-Jørgensen et al. 2002), and their dives often last only 9 -14 minutes (Heide-Jørgensen et al. 2002; Aoki et al. 2017). These diving patterns provide more opportunities for their detection by visual observers.

Deep-diving cetacean species are known to be vulnerable to anthropogenic sources of noise, including from the development of offshore energy. Active sonar and acoustic surveys such as seismic surveys

have been linked to numerous negative effects on these deep-diving species, including habitat displacement, disruption of biologically important behaviours (e.g. feeding attempts), masking of communication signals, chronic stress and potential auditory damage (Miller et al. 2009, Nowacek et al. 2015, McGeady et al. 2016, Stanistreet et al. 2022).

Quantifying the impacts of anthropogenic noise on deep diving cetacean species is difficult due to the lack of underlying data on their abundance and ecology. Offshore surveys for cetaceans are relatively expensive and resource-intensive compared with studying coastal species, and the cryptic behaviour of many deep-diving species often results in very low numbers of animals being recorded using typical survey methodology.

In recent years, several studies have combined data from multiple surveys to model the distribution of deep diving cetaceans in the north-eastern Atlantic (e.g. Rogan et al. 2017; Virgili et al. 2019; Breen et al. 2020). This approach can provide sufficient records of animals and allow the generation of density surfaces across the area of interest.

This study builds on the work done by Rogan et al. (2017) by modelling deep-diving cetacean data from a variety of sources, including from the three most recently available dedicated cetacean sighting surveys (SCANS-III, ObSERVE, NASS-2015), to provide the most comprehensive description of the distribution and abundance of beaked whales and other deep-diving cetaceans around Britain.

## 1.1 Project objectives

This project brings together data on deep-diving cetaceans from various surveys collected between 2005 and 2016. First, information from the most recent surveys (summer 2015-16) is collated and analysed to provide design-based estimates of abundance for each deep-diving species for which sufficient data are available. Second, the combined dataset (2005-2016) is used to model distribution in two ways: environmental drivers of deep-diver distribution are investigated using so-called explanatory models; and the best predicted density surfaces of abundance are generated from so-called predictive models.

## 1.2 Cetacean data sources

The project used data from a variety of sources.

The SCANS surveys are a series of large-scale cetacean surveys conducted in European Atlantic waters. They were initiated in 1994 in the North Sea and adjacent waters (SCANS 1995; Hammond et al. 2002) and continued in 2005, covering all shelf waters (SCANS-II 2008; Hammond et al. 2013), and 2007 in offshore waters (CODA 2009). In 2016, SCANS-III surveyed all waters covered by SCANS-II and CODA, except Irish waters (see below), (Hammond et al. 2021). The 1994 SCANS survey covered only shelf waters which are not typically home to deep diving species. No beaked whales were observed and there were unique sightings of only three pilot whale groups and two sperm whale groups. These data are not included in analysis here.

The study area, survey design and methods employed during the SCANS-II and SCANS-III surveys are described in Hammond et al. (2013) and Hammond et al. (2021), respectively. The CODA surveys are described in CODA (2009). All SCANS and CODA surveys were conducted in the summer, focused on

the month of July. SCANS surveys used a combination of ship and aerial platforms. CODA was conducted using ships.

In addition to collecting visual observations of cetaceans, some survey ships also collected acoustic data. Beaked whale detections from SCANS-II, CODA and SCANS-III were analysed by Quintana (2017), and these have also been included in this project.

The ObSERVE project conducted aerial surveys in Irish waters during the summer and winter of 2015 and 2016/17. Survey methods were equivalent to those used during the SCANS-III survey and are described in Rogan *et al*. (2018).

The North Atlantic Sightings Survey (NASS) is a series of mainly shipboard surveys conducted by Norway, Iceland, the Faroe Islands and Greenland in the central and eastern North Atlantic in summer (Lockyer & Pike 2009; Desportes et al. 2019). Data from the Faroes surveys in T-NASS 2007 (Pike *et al*. 2008) and NASS 2015 (Pike *et al*. 2019) were included in this project. The Faroes survey areas in T-NASS 2007 and NASS 2015 were contiguous with those of CODA and SCANS-III, respectively.

Survey effort from these surveys is shown in Figure 1. Note that effort from the North Sea area were included for estimation of abundance but excluded from distribution modelling (see also below).

Irrespective of source, only data collected in sea conditions of Beaufort 5 or below were included in the dataset for analysis. The resulting combined dataset was split into segments based on date, transect ID (where available) and sighting conditions, such that each segment should contain only effort from one day, only one transect and have been carried out by the same observers and under the same conditions. Segments ranged between 1 and 14.98 km long. For all data combined, this gave a total of 98,654 km effort for analysis (Table 1).

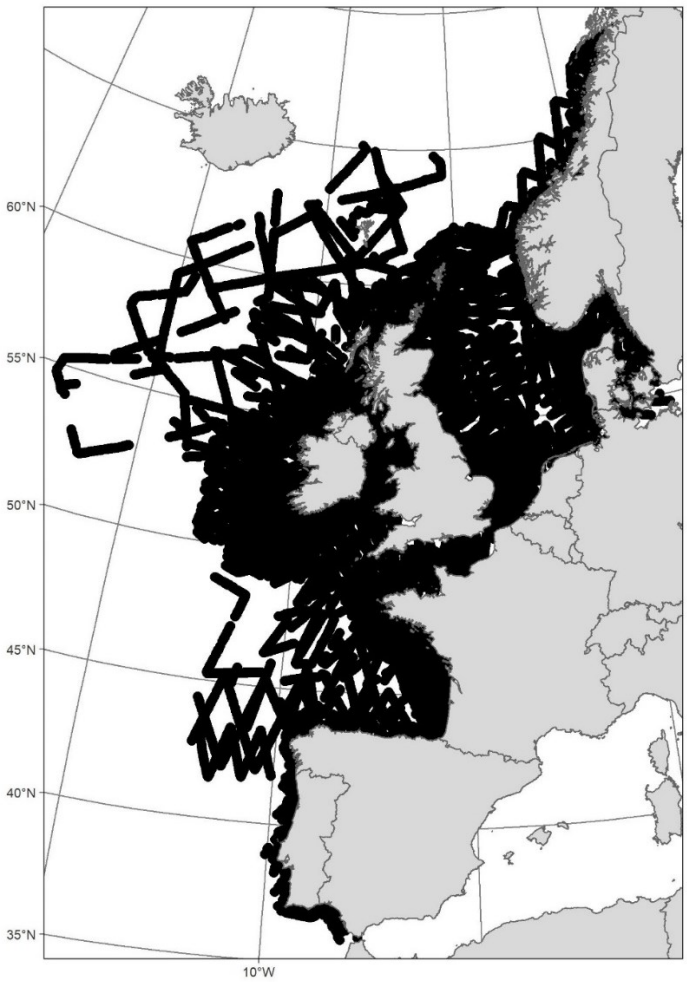


***Figure 1: Effort from designed surveys which contributed to the combined beaked whale dataset.***

***Table 1. Summary of the amount of effort and number of groups of animals detected on effort used in analysis for each of the data sources used. All beaked whale species includes sightings unidentified to species as well as those identified to species.***

| Source | Year | Total effort (km) | Pilot whale | Sperm whale | Northern bottlenose whale | Sowerby's beaked whale | Cuvier's beaked whale | All beaked whale species |
|---|---|---|---|---|---|---|---|---|
| SCANS-II | 2005 | 16,586 | 9 | 0 | 0 | 0 | 3 | 5 |
| CODA | 2007 | 19,355 | 43 | 31 | 0 | 7 | 6 | 28 |
| T-NASS | 2007 | 2,783 | 6 | | 12 | 0 | 0 | 12 |
| NASS | 2015 | 4,904 | 23 | 31 | 28 | 0 | 0 | 28 |
| ObSERVE | 2015-17 | 12,632 | 27 | 8 | 0 | 1 | 4 | 23 |
| SCANS-III - visual | 2016 | 35,013 | 55 | 18 | 2 | 2 | 8 | 42 |
| SCANS-III - acoustic | 2016 | 7,380 | 0 | 0 | 0 | 9 | 0 | 18 |

# 2 Estimates of abundance of deep-diving cetaceans in the European Atlantic in summer 2015-2016

Recent estimates of abundance of beaked whales, pilot whales and sperm whales in the European Atlantic are available from three major surveys: SCANS-III in summer 2016 (Hammond et al. 2021); ObSERVE in summer/winter 2015/2016 (Rogan et al. 2018); and the Faroes blocks of NASS in summer 2015 (Pike et al. 2019). Here we compile these estimates for SCANS-III (summer 2016), ObSERVE (summer 2016) and NASS (summer 2015) to generate the most up-to-date information on abundance of deep-diving cetacean species in this area.

The surveys were designed so that adjacent blocks shared a common boundary (i.e., were contiguous); consequently, estimates of abundance can be summed and no correction for overlapping areas is required (Figure 2).

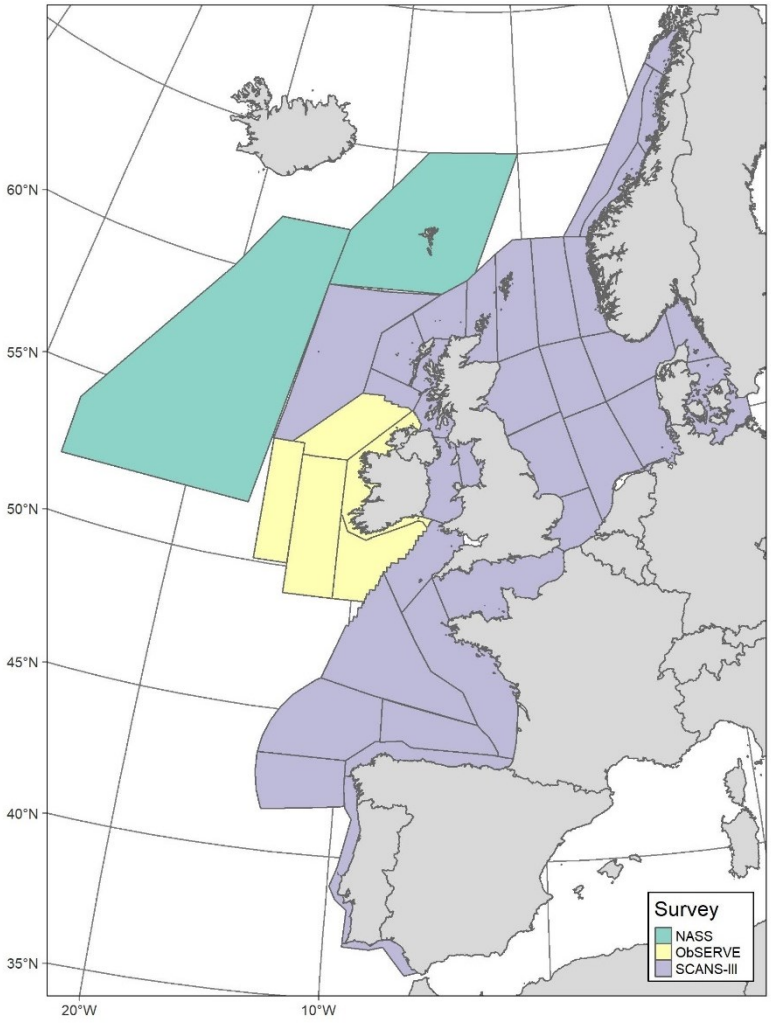


***Figure 2: Survey blocks for the SCANS-III, ObSERVE and NASS surveys. Blocks were designed to be contiguous.***

Summing estimates from NASS in 2015 and SCANS-III and ObSERVE in 2016 does not introduce bias in total estimated abundance but does lead to additional variance because animals may have moved between adjacent areas (in either direction) between years. No information is available to estimate

this additional variance, so our estimates of variance are negatively biased by an unknown amount. However, most estimates are in any case rather imprecise and additional variance is likely a minor contribution to total variance.

All published estimates of abundance presented here were calculated using design-based methods; full details are given in Hammond et al. (2021), Rogan et al. (2018) and Pike et al. (2019). In addition to collation of published estimates, additional analyses were conducted to obtain as much information from the data as possible, as described below. Calculations were made for each survey block for ship surveys and for each aerial survey (SCANS-III and ObSERVE) as a whole.

## 2.1 Sperm whale

Published estimates of abundance for sperm whale are available from the Faroes blocks of NASS 2015 (Pike et al. 2019) and the ship surveys of SCANS-III 2016 (Hammond et al. 2021). In addition, estimates were calculated from the small number of sightings made on the SCANS-III and the ObSERVE 2016 aerial surveys, using the effective strip width estimated for beaked whales in each case. These estimates are given in Table 2.

## 2.2 Pilot whale

Published estimates of abundance for pilot whale are available from the Faroes blocks of NASS 2015 (Pike et al. 2019), the ship and aerial surveys of SCANS-III 2016 (Hammond et al. 2021) and the ObSERVE 2016 aerial survey (Rogan et al. 2018). These estimates are given in Table 2.

## 2.3 Beaked whales

The available published estimates for beaked whales are limited to (a) northern bottlenose whale from NASS 2015 (Pike et al. 2019), (b) all beaked whales combined from SCANS-III (Hammond et al. 2021) and (c) all beaked whales combined, Cuvier's beaked whale and *Mesoplodon* spp from ObSERVE (Rogan et al. 2018).

Abundance of Cuvier's beaked whale, Sowerby's beaked whale, *Mesoplodon* spp and unidentified beaked whales from the SCANS-III shipboard survey was estimated using the effective strip width estimated for all beaked whales combined.

Abundance of northern bottlenose whale, Cuvier's beaked whale, Sowerby's beaked whale, and unidentified beaked whales from the SCANS-III aerial survey was derived from the estimate for all beaked whales combined based on the ratio of primary sightings:

$$\widehat{N}_{sp} = \hat{r}_{sp}\, \widehat{N}_{all}$$

where $N_{sp}$ is abundance of the species, $N_{all}$ is abundance of all beaked whales combined, and

$$\hat{r}_{sp} = \frac{n_{sp}}{n_{all}}$$

where $n_{sp}$ is the number of primary sightings of the species and $n_{all}$ is the number of primary sightings of all beaked whales combined.

The CV of the derived estimate was calculated as:

$$CV_{N_{sp}} = \sqrt{CV_{r_{sp}}^2 + CV_{N_{all}}^2}$$

where $CV_{r_{sp}}^2 = \frac{(1-\hat{r}_{sp})}{\hat{r}_{sp}\, n_{all}}$.

An estimate of the number of unidentified beaked whales for ObSERVE was derived by subtracting the estimates for Cuvier's beaked whale and *Mesoplodon* spp from the estimate of all beaked whales combined. Similarly, an estimate of the abundance of Gervais' beaked whale for SCANS-III ship surveys was calculated by subtracting the estimates for all identified species and unidentified beaked whales from the estimate of all beaked whales combined. The CVs of these estimates were calculated as for estimates based on the ratio of primary sightings, as described above.

These estimates are summarised in Table 2.

## 2.4 Allocating abundance of unidentified beaked whales to species

Estimates of abundance of unidentified beaked whales were then allocated to species based on the proportion of primary sightings of all identified species (including *Mesoplodon* spp) and added to estimates for species:

$$\widehat{N}_{adj} = \widehat{N}_{sp} + \hat{p}_{sp}\widehat{N}_{unid}$$

where $N_{adj}$ is abundance adjusted to include a proportion of unidentified beaked whale abundance, $N_{sp}$ is abundance of the species, $N_{unid}$ is abundance of unidentified beaked whales and

$$\hat{p}_{sp} = \frac{n_{sp}}{n_{id}}$$

where $n_{sp}$ is the number of primary sightings of the species and $n_{id}$ is the number of primary sightings of all identified beaked whales (i.e., excluding unidentified beaked whales).

The variance of the adjusted estimates was calculated by summing the variances of the species abundance and the proportion of the abundance from unidentified beaked whales so that

$$CV_{N_{adj}} = \frac{\sqrt{var\widehat{N}_{sp} + var\left(\hat{p}_{sp}\widehat{N}_{unid}\right)}}{\widehat{N}_{adj}}$$

where $var\left(\hat{p}_{sp}\widehat{N}_{unid}\right) = \hat{p}_{sp}^2\widehat{N}_{unid}^2\left(CV_{p_{sp}}^2 + CV_{N_{unid}}^2\right)$; and $CV_{p_{sp}}^2 = \frac{(1-\hat{p}_{sp})}{\hat{p}_{sp}\, n_{id}}$.

These calculations were made for northern bottlenose whale, Cuvier's beaked whale, Sowerby's beaked whale, Gervais' beaked whale and *Mesoplodon* spp, stratified by survey (NASS 2015, SCANS-III, ObSERVE), by survey type (aerial or ship) and by survey block for ship surveys.

Abundance estimates, including estimates adjusted for the addition of a proportion of unidentified beaked whale abundance are given in Table 2.

Summary estimates for 2015-16 for all species compared with those estimated for 2005-07 by Rogan et al. (2017) are given in Table 3.

*Table 2. Estimates of abundance of deep-diving cetacean species in the European Atlantic. All estimates derived from Hammond* et al. *(2017), Rogan* et al. *(2018) and Pike* et al. *(2019), corrected and calculated as described in the text. n = number of sightings. N = estimated abundance. D = estimated density. CV(N) = estimated co-efficient of variation of abundance and density. Lower/Upper 95% CL = lower/upper 95% confidence limit of abundance. N-unid = estimated abundance derived as a proportion of unidentified beaked whale abundance. N-adj = adjusted abundance (N + N-unid). D-adj = adjusted density.*

| Species | Survey | Block | n | N | D | CV(N) | Lower 95% CL | Upper 95% CL | N-unid | N-adj | D-adj | CV(N-adj) | Lower 95% CL | Upper 95% CL |
|---|---|---|---|---|---|---|---|---|---|---|---|---|---|---|
| **Sperm whale** | NASS-15 | Ship | 51 | 21,196 | 0.0832 | 0.569 | 7,511 | 59,816 | | | | | | |
| | SCANS-III | Aerial | 3 | 165 | 0.0001 | 0.376 | 81 | 337 | | | | | | |
| | SCANS-III | Ship | 38 | 13,518 | 0.0305 | 0.351 | 6,928 | 26,377 | | | | | | |
| | *SCANS-III* | *Total* | *41* | *13,683* | *0.0083* | *0.347* | *7,066* | *26,498* | | | | | | |
| | ObSERVE | Aerial | 5 | 637 | 0.0019 | 0.505 | 250 | 1,622 | | | | | | |
| **Sperm whale** | **Total** | | **97** | **35,517** | **0.0159** | **0.365** | **17,763** | **71,016** | | | | | | |
| **Pilot whale** | NASS-15 | Ship | 46 | 50,604 | 0.1986 | 0.393 | 24,079 | 106,348 | | | | | | |
| | SCANS-III | Aerial | 79 | 5,215 | 0.0043 | 0.605 | 1,745 | 15,583 | | | | | | |
| | SCANS-III | Ship | 37 | 20,657 | 0.0466 | 0.347 | 10,677 | 39,967 | | | | | | |
| | *SCANS-III* | *Total* | *116* | *25,872* | *0.0157* | *0.302* | *14,490* | *46,194* | | | | | | |
| | ObSERVE | Aerial | 20 | 7,413 | 0.0226 | 0.395 | 3,515 | 15,636 | | | | | | |
| **Pilot whale** | **Total** | | **182** | **83,889** | **0.0375** | **0.257** | **51,092** | **137,738** | | | | | | |
| **Northern bottlenose whale** | NASS-15 | Ship | 24 | 13,906 | 0.0546 | 0.784 | 3,579 | 54,035 | 0 | 13,906 | 0.0546 | 0.784 | 3,579 | 54,035 |
| | SCANS-III | Aerial | 2 | 175 | 0.0001 | 0.763 | 46 | 661 | 96 | 271 | 0.0002 | 0.571 | 96 | 250 |
| | SCANS-III | Ship | 0 | 0 | 0.0000 | | | | 0 | 0 | 0.0000 | | | |
| | *SCANS-III* | *Total* | *2* | *175* | *0.0001* | *0.763* | *46* | *661* | *96* | *271* | *0.0002* | *0.571* | *96* | *767* |
| | ObSERVE | Aerial | 0 | 0 | 0.0000 | | | | 0 | 0 | 0.0000 | | | |
| **Northern bottlenose whale** | **Total** | | **26** | **14,081** | **0.0063** | **0.775** | **3,673** | **53,989** | **96** | **14,177** | **0.0063** | **0.770** | **3,724** | **53,964** |

| Species | Survey | Block | n | N | D | CV(N) | Lower 95% CL | Upper 95% CL | N-unid | N-adj | D-adj | CV(N-adj) | Lower 95% CL | Upper 95% CL |
|---|---|---|---|---|---|---|---|---|---|---|---|---|---|---|
| **Cuvier's beaked whale** | NASS-15 | Ship | 0 | 0 | 0.0000 | | | | 0 | 0 | 0.0000 | | | |
| | SCANS-III | Aerial | 8 | 701 | 0.0006 | 0.456 | 299 | 1,641 | 382 | 1,083 | 0.0009 | 0.350 | 557 | 2,107 |
| | SCANS-III | Ship | 18 | 2,357 | 0.0053 | 0.482 | 962 | 5,777 | 503 | 2,860 | 0.0065 | 0.419 | 1,301 | 6,285 |
| | *SCANS-III* | *Total* | *26* | *3,058* | *0.0019* | *0.386* | *1,472* | *6,351* | *885* | *3,942* | *0.0024* | *0.318* | *2,144* | *7,249* |
| | ObSERVE | Aerial | 2 | 237 | 0.0007 | 0.712 | 68 | 832 | 147 | 384 | 0.0012 | 0.535 | 144 | 1,028 |
| **Cuvier's beaked whale** | **Total** | | **28** | **3,295** | **0.0015** | **0.362** | **1,656** | **6,556** | **1,032** | **4,327** | **0.0019** | **0.294** | **2,461** | **7,607** |
| **Sowerby's beaked whale** | NASS-15 | Ship | 0 | 0 | 0.0000 | | | | 0 | 0 | 0.0000 | | | |
| | SCANS-III | Aerial | 1 | 88 | 0.0001 | 1.040 | 16 | 469 | 48 | 135 | 0.0001 | 0.773 | 35 | 309 |
| | SCANS-III | Ship | 2 | 494 | 0.0011 | 0.955 | 102 | 2,393 | 476 | 970 | 0.0022 | 0.752 | 261 | 3,603 |
| | *SCANS-III* | *Total* | *3* | *582* | *0.0004* | *0.826* | *141* | *2,390* | *524* | *1,105* | *0.0007* | *0.667* | *337* | *3,628* |
| | ObSERVE | Aerial | 0 | 0 | 0.0000 | | | | 0 | 0 | 0.0000 | | | |
| **Sowerby's beaked whale** | **Total** | | **3** | **582** | **0.0003** | **0.826** | **141** | **2,390** | **524** | **1,105** | **0.0005** | **0.667** | **337** | **3,628** |
| **Gervais' beaked whale** | NASS-15 | Ship | 0 | 0 | 0.0000 | | | | 0 | 0 | 0.0000 | | | |
| | SCANS-III | Aerial | 0 | 0 | 0.0000 | | | | 0 | 0 | 0.0000 | | | |
| | SCANS-III | Ship | 1 | 29 | 0.0001 | 1.040 | 5 | 155 | 4 | 33 | 0.0001 | 0.941 | 7 | 155 |
| | *SCANS-III* | *Total* | *1* | *29* | *0.0000* | *1.040* | *5* | *155* | *4* | *33* | *0.0000* | *0.941* | *7* | *155* |
| | ObSERVE | Aerial | 0 | 0 | 0.0000 | | | | 0 | 0 | 0.0000 | | | |
| **Gervais' beaked whale** | **Total** | | **1** | **29** | **0.0000** | **1.040** | **5** | **155** | **4** | **33** | **0.0000** | **0.941** | **7** | **155** |
| ***Mesoplodon* spp** | NASS-15 | Ship | 0 | 0 | 0.0000 | | | | 0 | 0 | 0.0000 | | | |
| | SCANS-III | Aerial | 0 | 0 | 0.0000 | | | | 0 | 0 | 0.0000 | | | |
| | SCANS-III | Ship | 1 | 226 | 0.0005 | 1.197 | 36 | 1,434 | 182 | 408 | 0.0009 | 0.833 | 98 | 1,694 |
| | *SCANS-III* | *Total* | *1* | *226* | *0.0001* | *1.197* | *36* | *1,434* | *182* | *408* | *0.0002* | *0.833* | *98* | *1,694* |
| | ObSERVE | Aerial | 7 | 2,243 | 0.0068 | 0.682 | 668 | 7,531 | 515 | 2,758 | 0.0084 | 0.563 | 986 | 7,717 |
| ***Mesoplodon* spp** | **Total** | | **8** | **2,469** | **0.0011** | **0.629** | **796** | **7,657** | **697** | **3,166** | **0.0014** | **0.502** | **1,249** | **8,022** |

| Species | Survey | Block | n | N | D | CV(N) | Lower 95% CL | Upper 95% CL |
|---|---|---|---|---|---|---|---|---|
| **Unidentified beaked whale** | NASS-15 | Ship | 0 | 0 | 0.0000 | | | |
| | SCANS-III | Aerial | 6 | 526 | 0.0004 | 0.499 | 208 | 1,325 |
| | SCANS-III | Ship | 6 | 1,164 | 0.0026 | 0.712 | 332 | 4,087 |
| | *SCANS-III* | *Total* | *12* | *1,690* | *0.0010* | *0.515* | *653* | *4,370* |
| | ObSERVE | Aerial | 6 | 662 | 0.0020 | 0.499 | 263 | 1,669 |
| **Unidentified beaked whale** | **Total** | | **18** | **2,352** | **0.0011** | **0.396** | **1,114** | **4,966** |
| | | | | | | | | |
| **Beaked whales (all)** | NASS-15 | Ship | 24 | 13,906 | 0.0546 | 0.784 | 3,579 | 54,035 |
| | SCANS-III | Aerial | 17 | 1,489 | 0.0012 | 0.376 | 730 | 3,037 |
| | SCANS-III | Ship | 28 | 4,270 | 0.0096 | 0.378 | 2,086 | 8,741 |
| | *SCANS-III* | *Total* | *45* | *5,759* | *0.0035* | *0.297* | *3,259* | *10,177* |
| | ObSERVE | Aerial | 15 | 3,142 | 0.0096 | 0.505 | 1,235 | 7,997 |
| **Beaked whales (all)** | **Total** | | **84** | **22,807** | **0.0102** | **0.489** | **9,201** | **56,532** |

***Table 3. Estimates of abundance of deep-diving cetacean species in the European Atlantic for 2015-16 compared with estimates from 2005-07 from Rogan* et al. *(2017). n = number of sightings. N = estimated abundance. CV(N) = estimated co-efficient of variation of abundance. Lower/Upper 95% CL = lower/upper 95% confidence limit of abundance. adjusted = estimates adjusted to include a proportion of unidentified beaked whale abundance.***

| | 2005-07 | | | | | 2015-16 | | | | |
|---|---|---|---|---|---|---|---|---|---|---|
| **Species** | **n** | **N** | **CV(N)** | **Lower 95% CL** | **Upper 95% CL** | **n** | **N** | **CV(N)** | **Lower 95% CL** | **Upper 95% CL** |
| Sperm whale | 65 | 3,267 | 0.23 | 2,103 | 5,076 | 97 | 35,517 | 0.36 | 17,763 | 71,016 |
| Pilot whale | 59 | 172,195 | 0.35 | 88,194 | 336,206 | 182 | 83,889 | 0.26 | 51,092 | 137,738 |
| Northern bottlenose whale | 15 | 19,539 | 0.36 | 9,921 | 38,482 | 26 | 14,081 | 0.77 | 3,673 | 53,989 |
| *adjusted* | | *20,456* | *0.35* | *10,553* | *39,650* | | *14,177* | *0.77* | *3,724* | *53,964* |
| Cuvier's beaked whale | 17 | 2,286 | 0.48 | 942 | 5,552 | 28 | 3,295 | 0.36 | 1,656 | 6,556 |
| *adjusted* | | *4,471* | *0.51* | *1,735* | *11,519* | | *4,327* | *0.29* | *2,461* | *7,607* |
| Sowerby's beaked whale | 6 | 3,518 | 0.43 | 1,570 | 7,883 | 3 | 582 | 0.83 | 141 | 2,390 |
| *adjusted* | | *4,227* | *0.48* | *1,725* | *10,356* | | *1,105* | *0.67* | *337* | *3,628* |
| Gervais' beaked whale | | | | | | 1 | 29 | 1.04 | 5 | 155 |
| *Mesoplodon* spp | | | | | | 8 | 2,469 | 0.63 | 796 | 7,657 |
| Unidentified beaked whale | 25 | 3,811 | 0.26 | 2,322 | 6,254 | 18 | 2,352 | 0.40 | 1,114 | 4,966 |
| All beaked whales | 63 | 29,154 | 0.27 | 17,478 | 48,629 | 84 | 22,807 | 0.49 | 9,201 | 56,532 |

# 3 Distribution of deep-diving cetaceans

## 3.1 Modelling methods

Using the combined dataset, spatially referenced statistical models were developed to investigate the physical environmental features that best explained the distribution of deep-diving cetaceans. The candidate covariates considered for inclusion in the models are shown in Table 4, with some illustrated in Figure 3. Distribution plots of some of the covariates which were retained in models for any of the species are given in Appendix 1.

***Table 4. Covariate data considered for inclusion in the models of deep diving cetacean distribution.***

| Covariate name | Description | Unit of measurement | Data source |
|---|---|---|---|
| **X** | Longitude converted into UTM31 coordinate system | N/A | N/A |
| **Y** | Latitude converted into UTM31 coordinate system | N/A | N/A |
| **Depth** | Mean depth of the values assigned to effort making up the segment. Depth raster created using R package MARMAP (Pante and Simon-Bouhet 2013). | m | ETOPO1 database, hosted by NOAA (Amante and Eakins 2009). |
| **Standard deviation of depth (SD_depth)** | Standard deviation of depth calculated over a buffer of 5km radius. Depth raster created using R package MARMAP (Pante & Simon-Bouhet, 2013). Analysis of raster conducted using R package RASTER (Hijmans, 2020) | m | ETOPO1 database, hosted by NOAA (Amante & Eakins, 2009). |
| **Slope** | Seabed gradient, extracted from a single point location using depth data extracted using R package MARMAP (Pante and Simon-Bouhet 2013). Analysis of raster conducted using R package RASTER (Hijmans, 2020) | (°) | ETOPO1 database, hosted by NOAA (Amante & Eakins, 2009). |
| **Aspect** | Slope facing direction. Extracted from a single point location using R package MARMAP (Pante & Simon-Bouhet, 2013). Analysis of raster conducted using R package RASTER (Hijmans, 2020) | (°) | ETOPO1 database, hosted by NOAA (Amante & Eakins, 2009). |
| **Surface salinity (SAL)** | Sea water salinity | PSU | GLORYS12V1: a reanalysis of the Copernicus Marine Environment Monitoring Service (CMEMS) global ocean eddy-model, based largely on the current real-time global forecasting CMEMS system. Downloaded from https://resources.marine.copernicus.eu/ (Fernandez and Lellouche 2021) |
| **Mixed Layer Depth (MLD)** | Ocean mixed layer depth. The depth where the density increase compared to density at 10m depth corresponds to | m | GLORYS12V1: a reanalysis of the Copernicus Marine Environment Monitoring Service (CMEMS) global |

| | | | |
|---|---|---|---|
| | a temperature decrease of 0.2°C in local surface conditions | | ocean eddy-model, based largely on the current real-time global forecasting CMEMS system. Downloaded from https://resources.marine.copernicus.eu/ (Fernandez & Lellouche, 2021) |
| **Sea surface temperature (SST)** | Optimally Interpolated (OI) merged microwave-infrared SST product from Remote Sensing Systems. | °C | This is the Optimally Interpolated (OI) merged microwave-infrared SST product from the Advanced Very High-Resolution Radiometer (AVHRR) instrument. Data provided by NEODAAS (Casey et al. 2010) |
| **Sea bottom temperature (SBT)** | Sea water potential temperature at sea floor | °C | GLORYS12V1: a reanalysis of the Copernicus Marine Environment Monitoring Service (CMEMS) global ocean eddy-model, based largely on the current real-time global forecasting CMEMS system. Downloaded from https://resources.marine.copernicus.eu/ (Fernandez and Lellouche 2021) |
| **Sea surface Height (SSH)** | Sea surface height above the ellipsoid. SSH is the difference between the actual sea surface height at any given time and place, and that which it would have if the ocean were at rest. SSH = geoid +ADT | m | GLORYS12V1: a reanalysis of the Copernicus Marine Environment Monitoring Service (CMEMS) global ocean eddy-model, based largely on the current real-time global forecasting CMEMS system. Downloaded from https://resources.marine.copernicus.eu/ (Fernandez and Lellouche 2021) |
| **Distance from 1000m isobath** | Distance at shortest point | km | ETOPO1 database, hosted by NOAA (Amante & Eakins, 2009). |
| **Distance from 2000m isobath** | Distance at shortest point | km | ETOPO1 database, hosted by NOAA (Amante & Eakins, 2009). |
| **Distance from canyons** | Distance at shortest point. Canyons are deep, narrow valleys with steep sides. | km | Seafloor Geomorphic Features map (Harris et al. 2014) |
| **Distance from escarpments** | Distance at shortest point. Escarpment is the bottom of a cliff or steep slope. | km | Seafloor Geomorphic Features map (Harris et al. 2014) |
| **Distance from fans** | Distance at shortest point. Fans are triangle-shaped deposits of sediment usually created as flowing water interacts with mountains, hills, or the steep walls of canyons. | km | Seafloor Geomorphic Features map (Harris et al. 2014) |
| **Distance from ridges** | Distance at shortest point. Ridges are chains of mountains that form a continuous elevated crest | km | Seafloor Geomorphic Features map (Harris et al. 2014) |
| **Distance from seamounts** | Distance at shortest point. Seamounts are isolated rises in elevation of 1000m or more from the surrounding seafloor. | km | Seafloor Geomorphic Features map (Harris et al. 2014) |
| **Distance from troughs** | Distance at shortest point. A trough is a linear depression extending over a distance. Shallower than a canyon. | km | Seafloor Geomorphic Features map (Harris et al. 2014) |

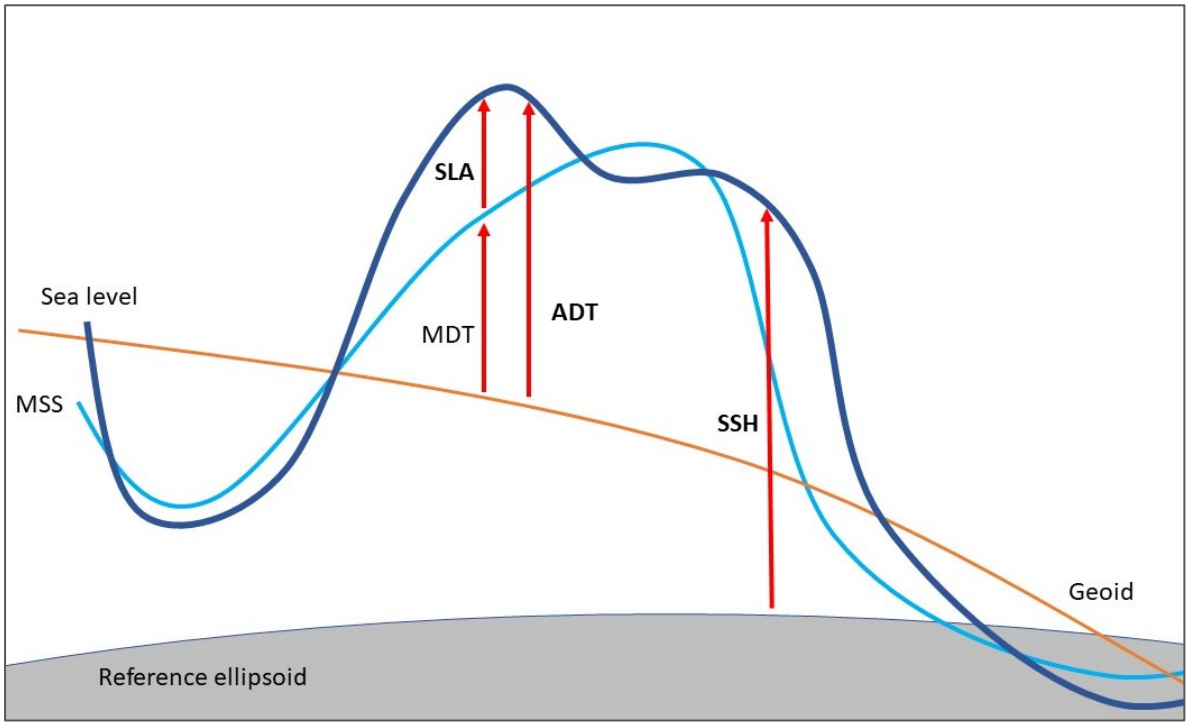


**Reference ellipsoid**: smoothed mathematical representation of Earth's sea level surface, ignoring the effects of tides, seasonal currents, and waves.
**Geoid**: the shape that the ocean surface would take under the influence of gravity and the earth's rotation, assuming other influences such as tide and wind were absent.
**MSS:** 20-year Mean Sea Surface above the ellipsoid.
**SLA**: Sea level anomaly (difference between MSS and sea level at time of measurement).
**MDT**: Mean Dynamic Topography: mean departure of the sea surface from the geoid due to ocean dynamics.
**ADT**: Absolute Dynamic Topography: departure of the sea surface from the geoid due to ocean dynamics. ADT = MDT+SLA.
**SSH**: Sea Surface Height: height of the sea surface above the ellipsoid.

***Figure 3. Schematic showing the differences between the different measures of mesoscale activity SLA, ADT and SSH with reference to the geoid. Adapted from Fernandez & Lellouche (2021).***

### 3.1.1 Model structure, fitting and selection

Modelling methods followed the GAM framework previously outlined in Gilles et al. (2016), Becker et al. (2016, 2017) and Rogan et al. (2017). Tweedie and negative binomial distributions were considered as candidate error structures to account for over-dispersion in the cetacean count data. The negative binomial distribution is a generalisation of a Poisson regression, which loosens the assumption that variance is equal to the mean. This is often used to model counts, particularly for count data which are over-dispersed – that is, contain greater variability than would be expected (Jain and Consul 1971). The Tweedie is a family of exponential type distributions, which are tolerant to large numbers of zero observations (Candy 2004).

The general structure of the model, using a logarithmic link function, was:

$$n_i = exp\left[\ln(a_i) + \theta_0 + \sum f_k(z_{ik})\right]$$

where $n_i$ is the number of individuals detected in the $i^{th}$ effort segment, the offset $a_i$ is the effective area searched (segment length * (2 * estimated effective strip width) for the $i^{th}$ segment, $\theta_0$ is the intercept, $f_k$ are smoothed functions of the explanatory environmental covariates, and $z_{ik}$ is the value of the $k^{th}$ explanatory covariate in the $i^{th}$ segment. Estimated effective strip widths were available from previous analysis for all the dedicated survey data (CODA 2009; Hammond et al. 2013, 2021; Rogan et al. 2017, 2018; Pike et al. 2008, 2019).

Smooth functions were fitted using restricted maximum likelihood (REML) with automatic term selection (Marra and Wood 2011). Thin-plate regression splines were used for all covariates except for Aspect for which a cyclic penalized cubic regression spline was used. This method was used for model fitting because it helps to avoid overfitting of the smooth functions by including a modification to penalize slightly the null space. The method can reduce the estimated degrees of freedom of a covariate term to one or less, and even to zero if it does not contribute sufficiently to explaining the variability in the data. Following initial fitting of a model including all candidate covariates, those covariates with estimated degrees of freedom of 0.1 or less were removed from the model. Selection among models was based on Akaike's Information Criterion (AIC). Goodness of fit of models was assessed by inspection of QQ plots and plots of model residuals.

The data on distance to various features (Table 4) were correlated to an extent that depended on the dataset being modelled. Correlated covariates should not be included in the same model. To select which of the correlated covariates should be included in the model in each instance, they were first modelled independently and the covariate resulting in the lowest AIC value was taken forward for use in subsequent modelling.

Two types of model were fitted. So-called predictive models included geographical coordinates (X, Y – see Table 4) as well as environmental covariates. Models including XY covariates typically perform best at describing the current distribution of a species from a particular dataset, but may perform less well at predicting patterns in distributions over time due to the amount of variability usually explained by the XY covariates (Lambert et al. 2014). Relationships between animal density and environmental covariates that may help explain distribution are likely to be influenced by inclusion of geographical coordinates. Consequently, so-called explanatory models, that excluded geographical coordinates, were also fitted to investigate environmental drivers of distribution.

Apart from the inclusion or exclusion of geographical coordinates, modelling implementation was the same for explanatory models and predictive models. For each type of model, a minimum of two models were fitted per species. Firstly, a model including only static covariates (depth, aspect, the best "distance to" covariate as determined by AIC, the best of SD depth and slope as determined by AIC – Table 4) was fitted. Secondly, a model that also included dynamic covariates (Table 4) was fitted.

Note that the dataset used for modelling excluded the shallow waters of the North Sea area, which is not suitable habitat for deep diving species (Figure 4). Note also that the number of effort segments used for modelling was species dependent because some covariates were removed to reduce the number of effort segments with missing values and which covariates were removed depended on which "distance to" and monthly dynamic covariate was selected.

Estimated density from the most supported model for each species was predicted onto a grid covering the study area. Note that the area used for model predictions is slightly larger than the area covered

by the surveys, excluding the North Sea area (Figure 4). This prediction area was selected to incorporate areas of similar habitat to those surveyed, and to provide a more rounded prediction area. When model predictions were made, only those grid cells with covariate values within the range of covariate values included in the survey data were used for the prediction.

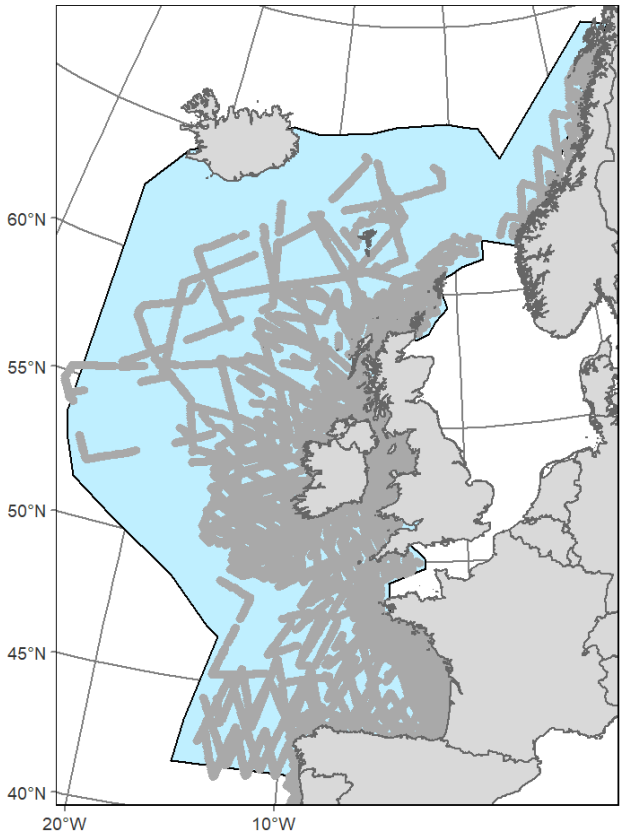


***Figure 4. Area covered by the prediction grid used in the modelling, overlaid on the survey effort included in the modelling..***

## 3.2 Results of models to investigate environmental drivers of distribution

The negative binomial distribution was found to best describe the error structure of the data for all species. Although both explanatory and predictive models were fitted to all species, the only predictive model presented below is for all beaked whales combined. For Sowerby's beaked whale, the fitted predictive model including the XY 2-D smooth function was unable to generate a useable spatial prediction of density. For all other species, the XY covariate was not retained when included as a candidate in the model, so the predictive model was the same as the explanatory model.

### 3.2.1 All beaked whale species combined – explanatory model

This analysis included acoustic detections of Sowerby's beaked whale and sightings of Cuvier's beaked whale, Sowerby's beaked whale, Gervais' beaked whale and northern bottlenose whale, as well as sightings and acoustic detections of beaked whales which could not be attributed to species.

There were 10,605 modelled survey effort segments for all beaked whales combined. Of these, 140 (1.3 %) segments contained at least one beaked whale sighting or acoustic detection.

The model including dynamic covariates performed best. Distance to escarpments was selected by AIC as the best seabed covariate to take forward into the model along with depth, sea surface temperature and mixed layer depth, although mixed layer depth was not retained in the best model.

Table 5 and Figure 5 give the model results, including plots of the partial effect on density of the fitted smooth function for each model covariate. QQ and residuals plots are shown in Appendix 2. Figure 6 shows the distribution of density predicted from the model.

Depth was an important covariate for beaked whales, with higher density predicted in waters greater than 1000m in depth. Density was also predicted to be higher in sea surface temperatures cooler than around 12°C and warmer than around 20°C.

***Table 5. Results of the best explanatory model for all beaked whales combined.***

| Error distribution | Model covariates | Estimated degrees of freedom | % Deviance explained | Model degrees of freedom |
|---|---|---|---|---|
| **Negative binomial** | Depth | 5.71 | 28.7 | 11.9 |
| | Distance to escarpments | 0.76 | | |
| | SST | 3.73 | | |

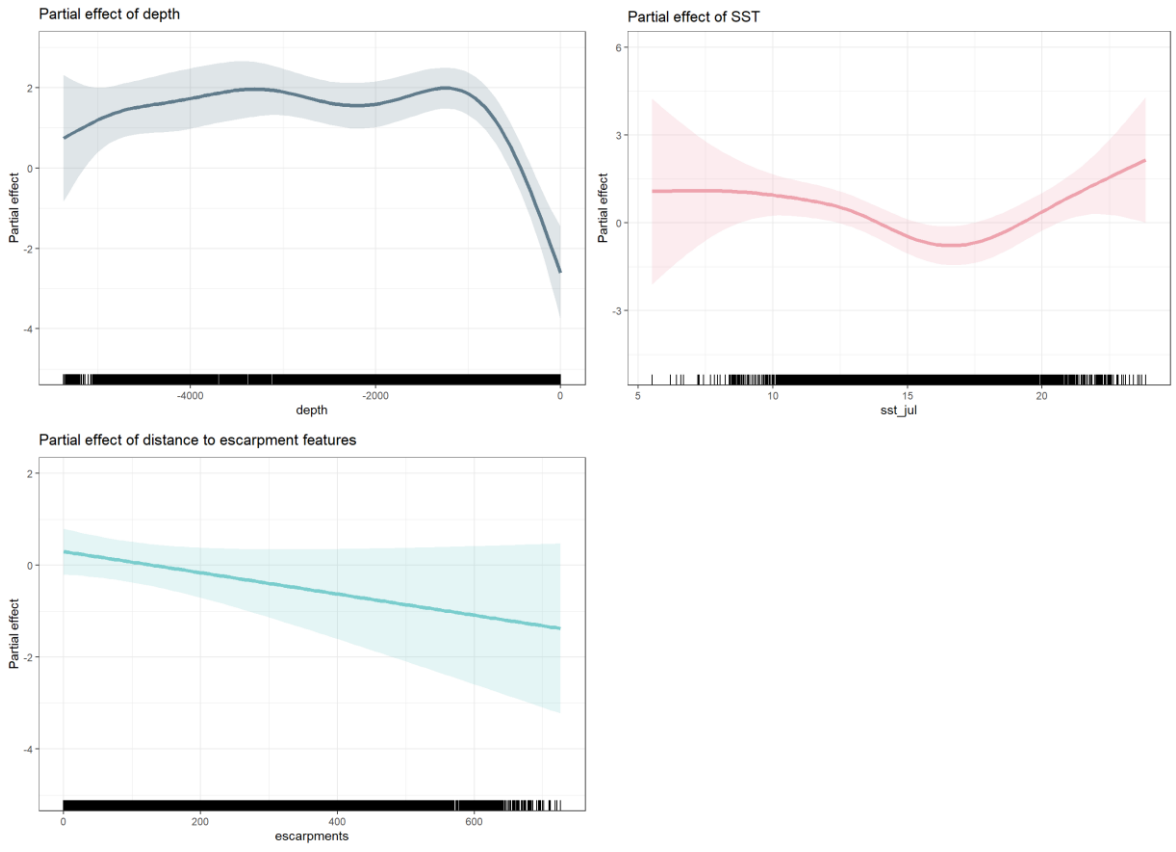


***Figure 5. Plots of the partial effect on density of covariates retained in the best explanatory model of all beaked whales combined.***

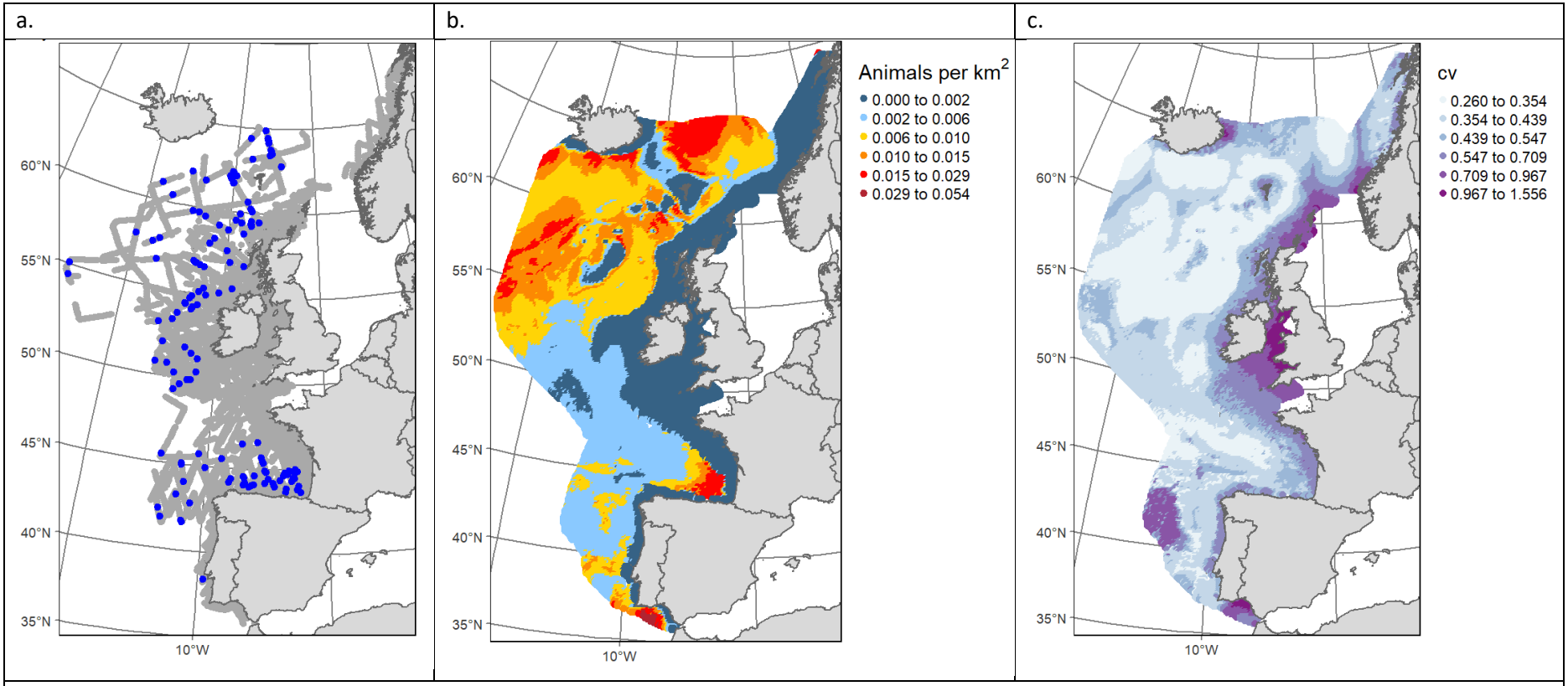


***Figure 6. (a) modelled effort and detections, (b) predicted density surface and (c) estimated CV surface for the best explanatory model for all beaked whales combined.***

### 3.2.2 All beaked whales combined – predictive model including XY covariates

The modelling process for predictive models was the same as for the explanatory models except that X and Y geographical covariates (Table 4) were included in the models as a 2-D isotropic smooth function along with other environmental covariates.

This analysis included acoustic detections of Sowerby's beaked whale and sightings of Cuvier's beaked whale, Sowerby's beaked whale, Gervais' beaked whale and northern bottlenose whale, as well as sightings and acoustic detections of beaked whales which could not be attributed to species.

There were 10,605 modelled survey effort segments for all beaked whales combined. Of these, 143 (1.3 %) segments contained at least one beaked whale sighting or acoustic detection.

The model including dynamic covariates was assessed to be the best. Depth and sea surface height were the only covariates retained by the model in addition to geographical coordinates X, Y, modelled as a 2-dimensional isotropic smooth function.

Table 6 and Figure 7 give the model results, including plots of the partial effect on density of the fitted smooth function for each model covariate. QQ and residuals plots are shown in Appendix 2. Figure 8 shows the distribution of density predicted from the model.

The X, Y component of the model predicted higher density to the northwest. In addition, density was predicted to be higher in waters greater than 1000m in depth and to increase with increasing sea surface height.

***Table 6. Results of the best predictive model for all beaked whales combined.***

| Error distribution | Model covariates | Estimated degrees of freedom | % Deviance explained | Model degrees of freedom |
|---|---|---|---|---|
| **Negative binomial** | X,Y | 15.45 | 35.9 | 22.6 |
| | Depth | 5.22 | | |
| | Sea surface height | 0.88 | | |

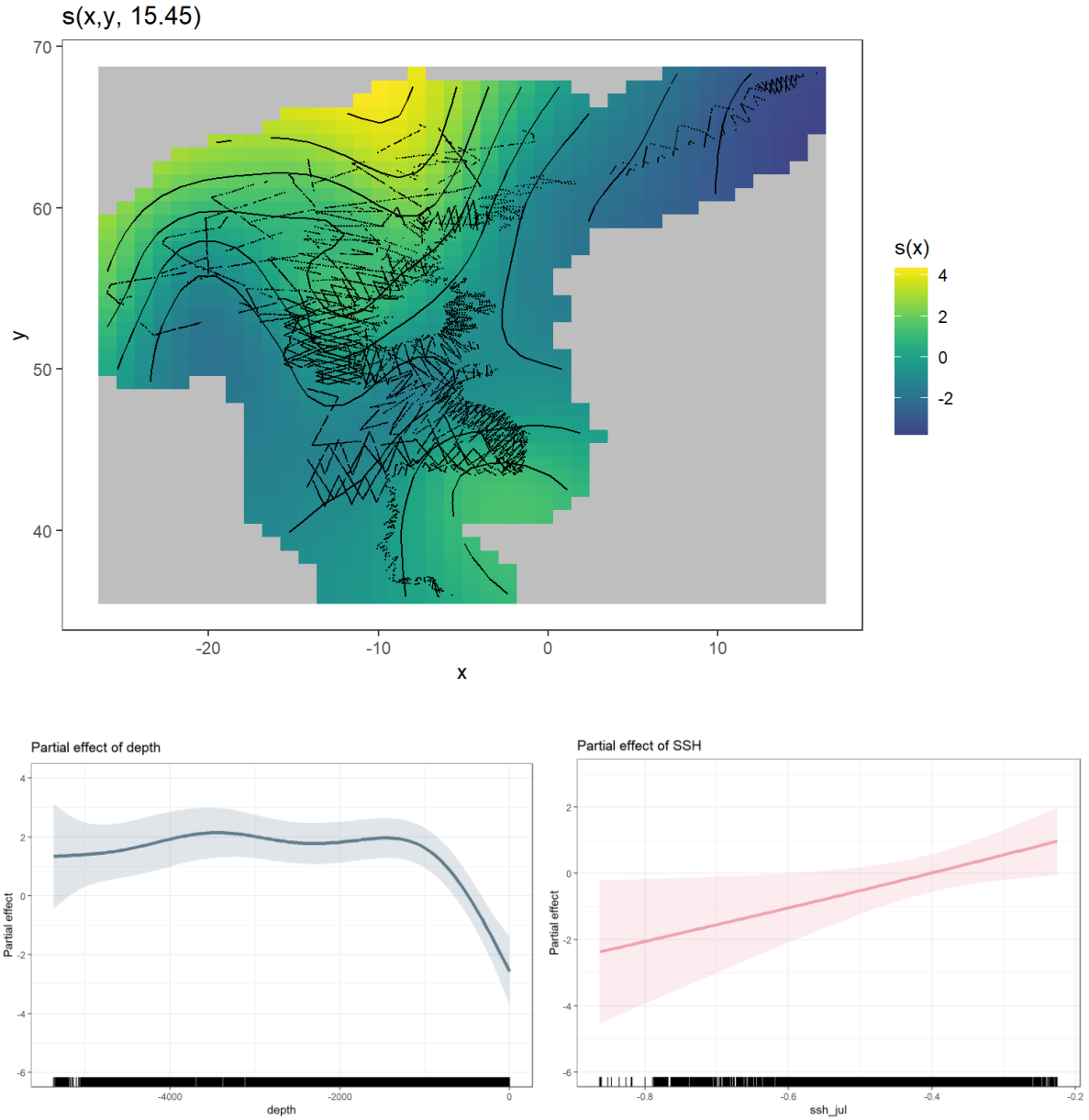


***Figure 7. Plots of the partial effect on density of covariates retained in the best predictive model for all beaked whales combined.***

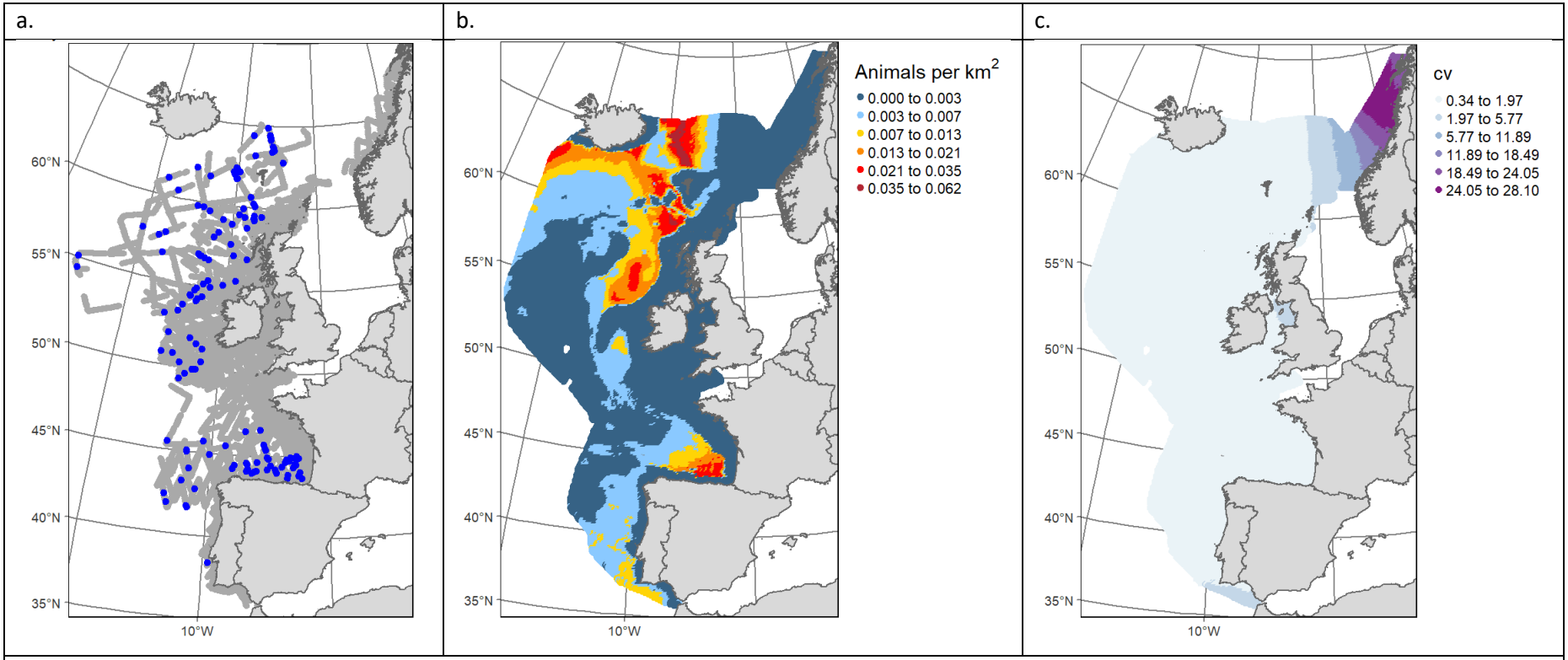


***Figure 8. (a) modelled effort and detections, (b) predicted density surface and (c) estimated CV surface for the best predictive model for all beaked whales combined.***

### 3.2.3 Sowerby's beaked whale – explanatory model

This analysis included visual and acoustic detections that were recorded as Sowerby's beaked whale.

There were 10,605 modelled survey effort segments for Sowerby's beaked whale. Of these, only 16 (0.15 %) segments contained one or more Sowerby's beaked whale sighting or acoustic detection.

The best model included dynamic covariates, and the final model retained sea bottom temperature and sea surface height.

Table 7 and Figure 9 give the model results, including plots of the partial effect on density of the fitted smooth function for each model covariate. QQ and residuals plots are shown in Appendix 2. Figure 10 shows the distribution of density predicted from the model.

Density was predicted to increase linearly with increasing sea surface height. The sea bottom temperature with the highest predicted density was $6^0$C, with predicted density decreasing at both higher and lower temperatures. The confidence intervals at temperatures higher than $6^0$C become increasingly wide.

***Table 7. Results of the best explanatory model for Sowerby's beaked whale.***

| Error distribution | Model covariates | Estimated degrees of freedom | % Deviance explained | Model degrees of freedom |
|---|---|---|---|---|
| **Negative binomial** | Sea bottom temperature | 2.93 | 50.3 | 4.8 |
| | Sea surface height | 0.89 | | |

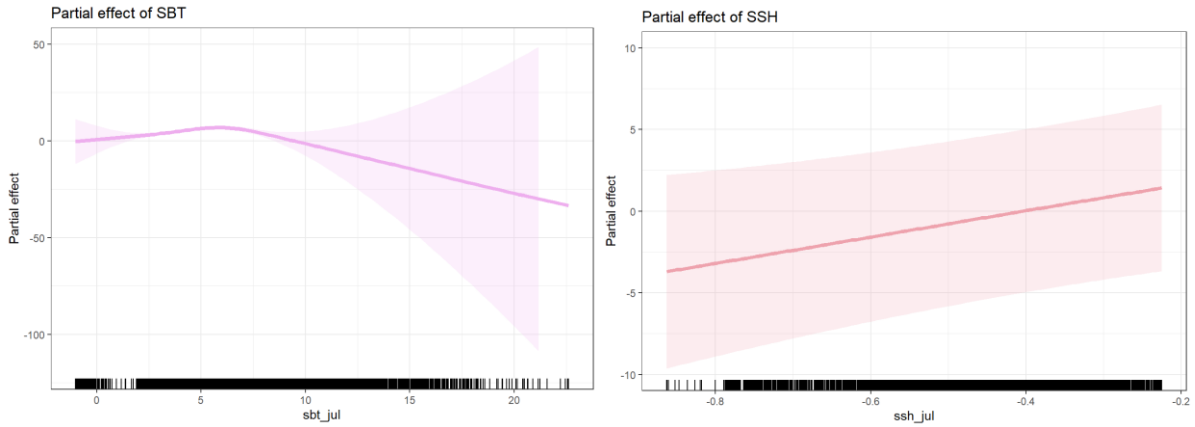


***Figure 9. Plots of the partial effect on density of covariates retained in the best explanatory model for Sowerby's beaked whale.***

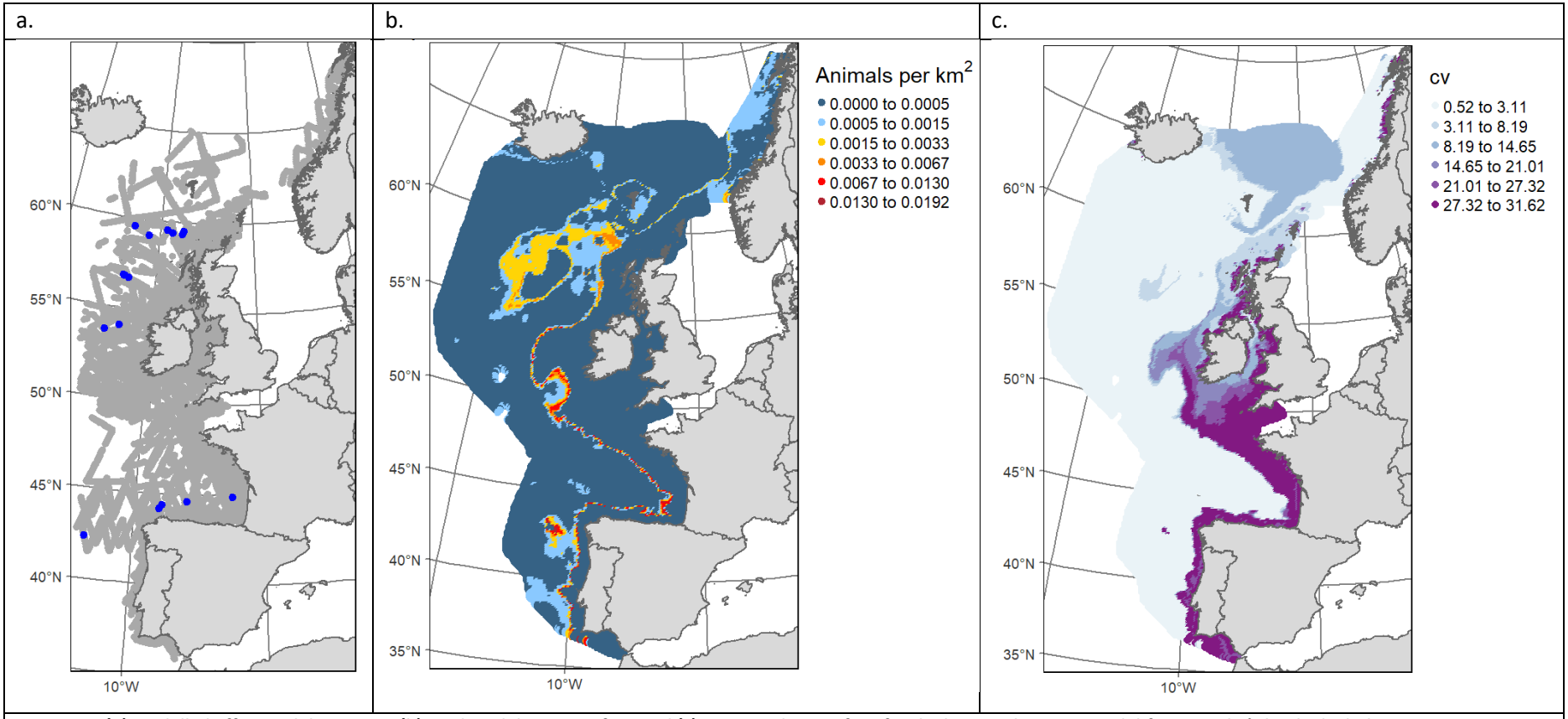


***Figure 10. (a) modelled effort and detections, (b) predicted density surface and (c) estimated CV surface for the best explanatory model for Sowerby's beaked whale.***

### 3.2.4 Northern bottlenose whale – explanatory model

This analysis included visual detections recorded as northern bottlenose whale; there were no acoustic detections of this species.

There were 8,936 modelled survey effort segments for northern bottlenose whale. Of these, 41 (0.45 %) segments contained one or more sighting.

The best model was that using only static covariates, with the final model retaining depth, aspect and distance from fans (Table 4).

Table 8 and Figure 11 give the model results, including plots of the partial effect on density of the fitted smooth function for each model covariate. QQ and residuals plots are shown in Appendix 2. Figure 12 shows the distribution of density predicted from the model.

Higher density was predicted at depths greater than around 500m and distances from fans greater than around 500km. The relationship with aspect is weak but shows a slight increase in density in areas with an approximate east facing (900) slope.

When running the predictive model for this species, the geographical covariates X, Y were not retained. Thus, the explanatory model serves as both predictive and explanatory models.

***Table 8. Results of the best explanatory model for northern bottlenose whale.***

| Error distribution | Model covariates | Estimated degrees of freedom | % Deviance explained | Model degrees of freedom |
|---|---|---|---|---|
| **Negative binomial** | Aspect | 0.59 | 56.8 | 10.9 |
| | Depth | 5.50 | | |
| | Distance to fan features | 3.89 | | |

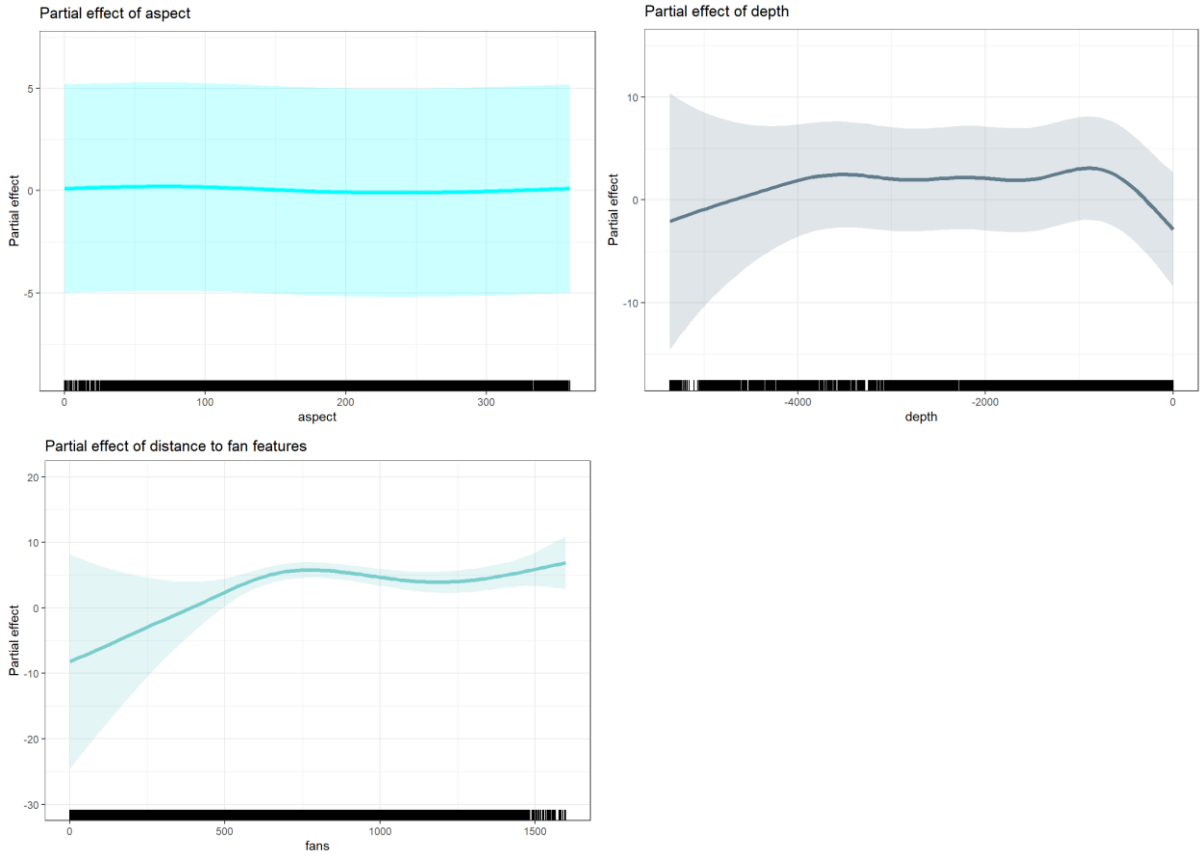


***Figure 11. Plots of the partial effect on density of covariates retained in the best explanatory model of northern bottlenose whale.***

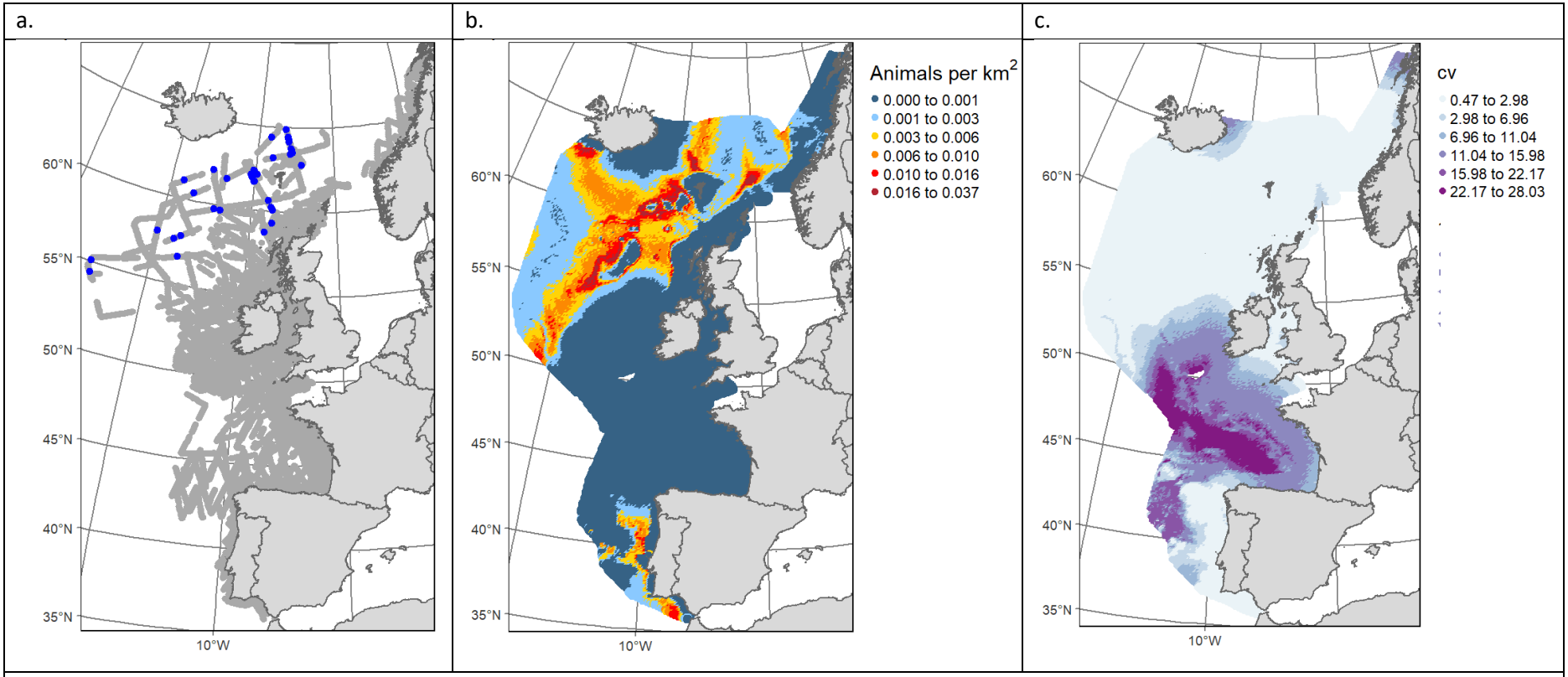


***Figure 12. (a) modelled effort and detections, (b) predicted density surface and (c) estimated CV surface for the best explanatory model for northern bottlenose whale.***

### 3.2.5 Cuvier's beaked whale – explanatory model

This analysis included visual detections recorded as Cuvier's beaked whale; there were no acoustic detections of this species.

There were 7,891 modelled survey effort segments for Cuvier's beaked whale. Of these, 17 (0.22%) segments contained one or more sighting.

The best model included dynamic covariates and retained depth and mixed layer depth in March.

Table 9 and Figure 13 give the model results, including plots of the partial effect on density of the fitted smooth function for each model covariate. QQ and residuals plots are shown in Appendix 2. Figure 14 shows the distribution of density predicted from the model.

Density was predicted to increase linearly with depth and with increasing seabed variability (SD depth). Density was predicted to decline at increasing distances from escarpment features.

As with northern bottlenose whale, the geographical covariates X, Y were not retained. Thus, the explanatory model serves as both predictive and explanatory models.

***Table 9. Results of the best explanatory model for Cuvier's beaked whale.***

| Error distribution | Model covariates | Estimated degrees of freedom | % Deviance explained | Model degrees of freedom |
|---|---|---|---|---|
| **Negative binomial** | Depth | 0.97 | 26.6 | 3.01 |
| | Distance to escarpments | 0.48 | | |
| | SD depth | 0.56 | | |

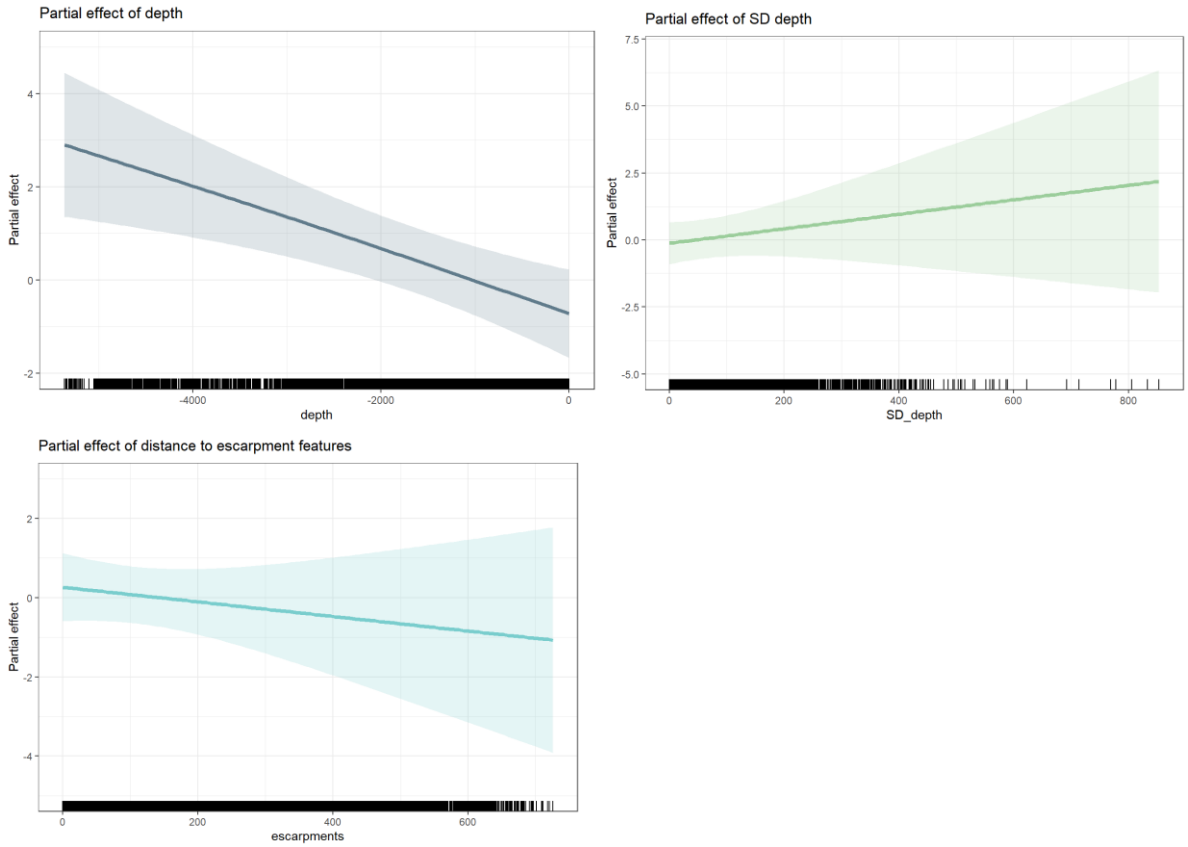


***Figure 13. Plots of the partial effect on density of covariates retained in the best explanatory model for Cuvier's beaked whale.***

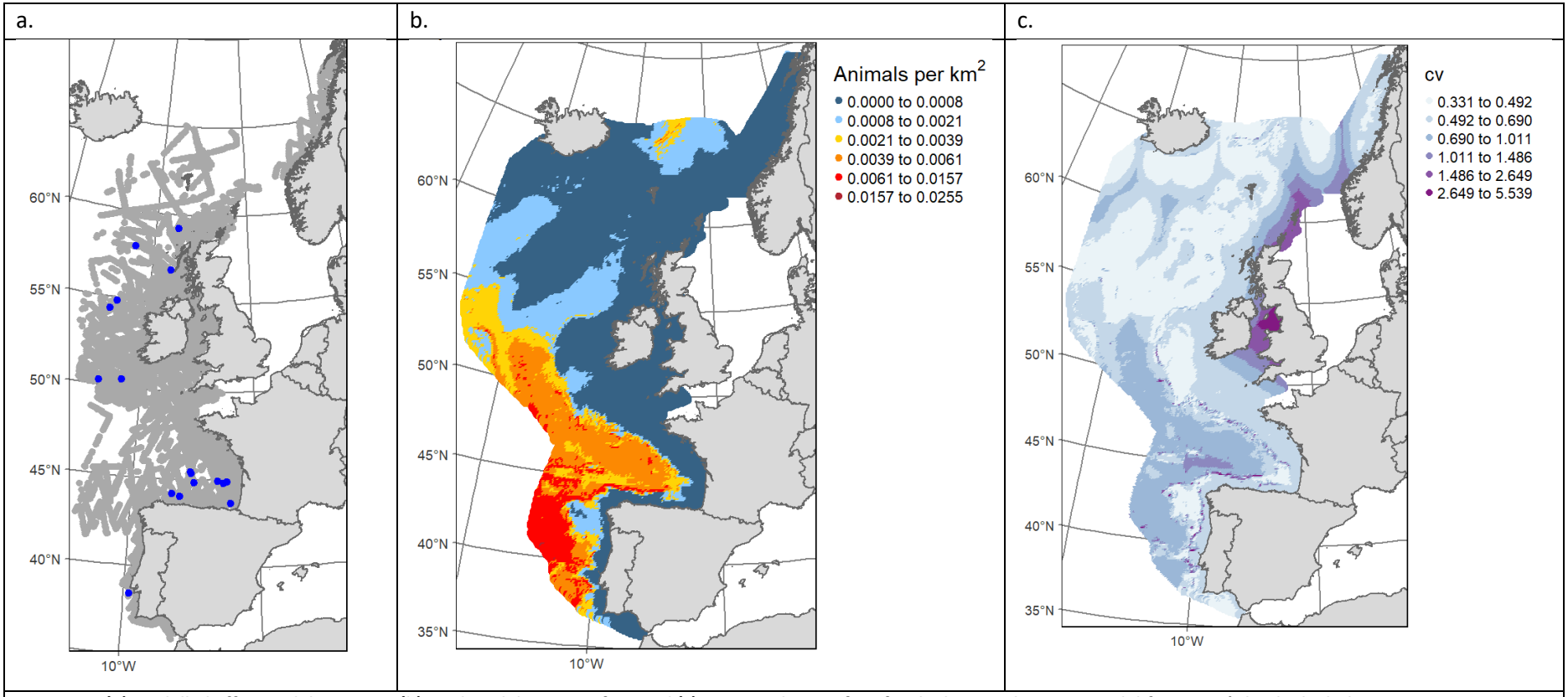


***Figure 14. (a) modelled effort and detections, (b) predicted density surface and (c) estimated CV surface for the best explanatory model for Cuvier's beaked whale.***

### 3.2.6 Sperm whale – explanatory model

This analysis included visual detections recorded as sperm whale; there were no acoustic detections of this species.

There were 7,891 modelled survey effort segments for sperm whale. Of these, 64 (0.81%) segments contained one or more sighting.

The best model included dynamic covariates and retained sea bottom temperature and depth of mixed layer, as well as distance to escarpment features.

Table 10 and Figure 15 give the model results, including plots of the partial effect on density of the fitted smooth function for each model covariate. QQ and residuals plots are shown in Appendix 2. Figure 16 shows the distribution of density predicted from the model.

Sea bottom temperature was the only covariate that showed much of a relationship with sperm whale density, with higher predicted density at temperatures around 5°C. Whilst other covariates were retained in the model, they have very wide confidence intervals, and do not show strong relationships.

Similarly to northern bottlenose whale and Cuvier's beaked whale, when running the predictive model for this species, the geographical covariates X, Y were not retained. Thus, the explanatory model serves as both predictive and explanatory models.

***Table 10. Results of the best explanatory model for sperm whale.***

| Error distribution | Model covariates | Estimated degrees of freedom | % Deviance explained | Model degrees of freedom |
|---|---|---|---|---|
| **Negative binomial** | Sea bottom temperature | 3.33 | 35 | 5.04 |
| | Distance to escarpments | 0.33 | | |
| | Mixed layer depth | 0.39 | | |

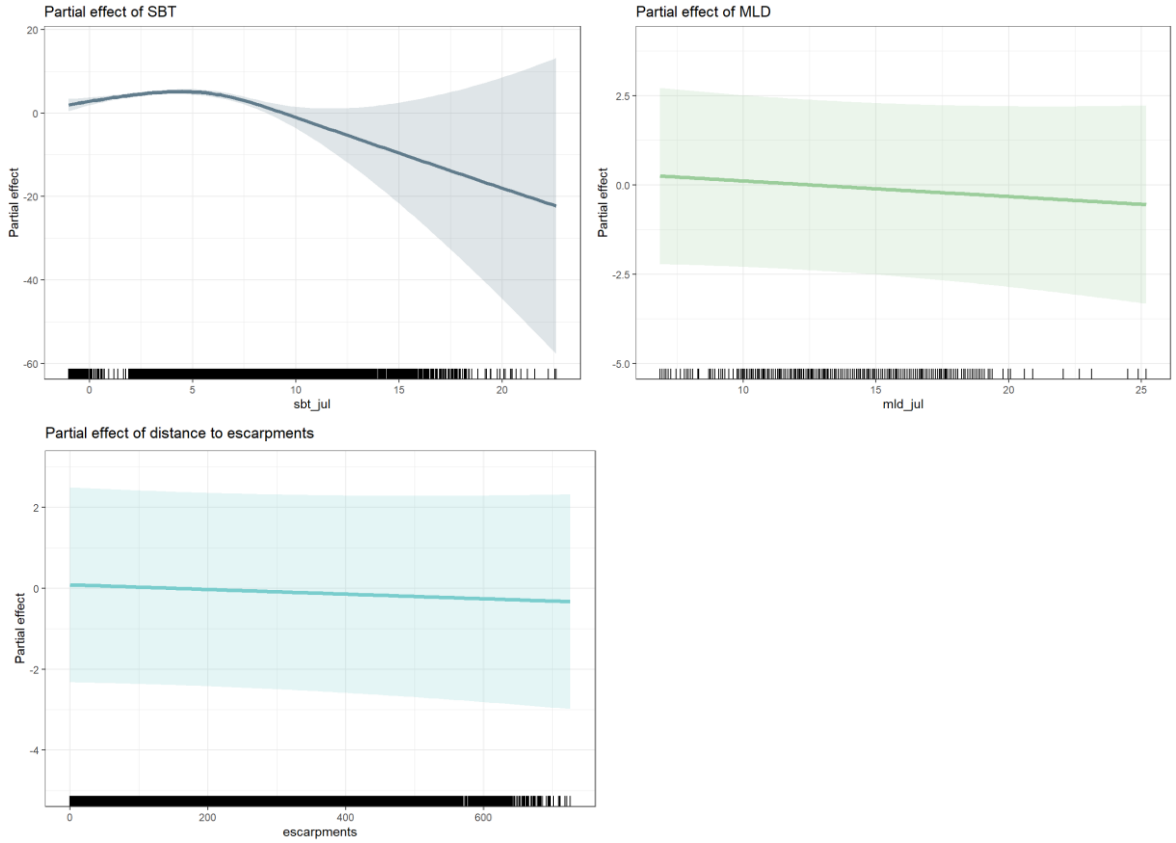


***Figure 15. Plots of the partial effect on density of covariates retained in the best explanatory model for sperm whale.***

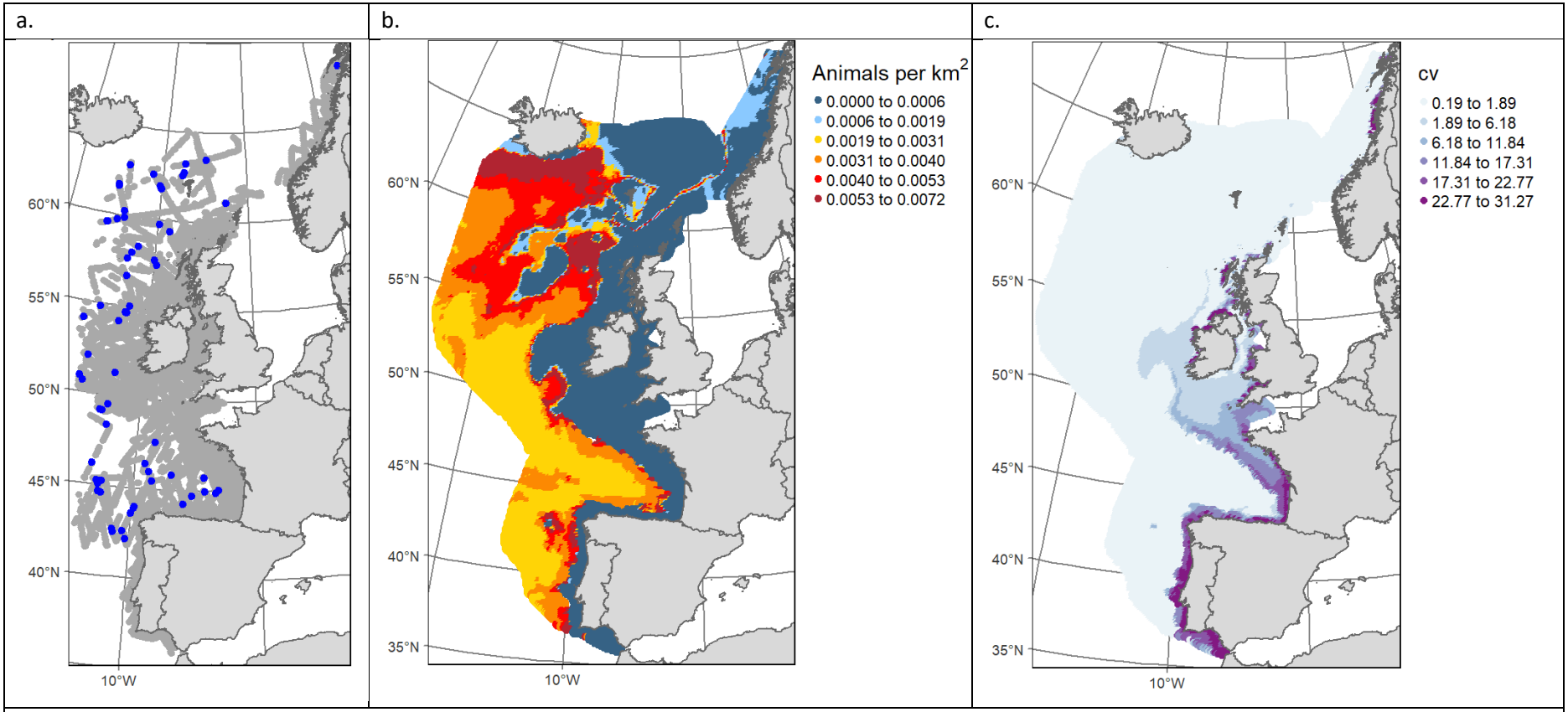


***Figure 16. (a) modelled effort and detections, (b) predicted density surface and (c) estimated CV surface for the best explanatory model for sperm whale.***

### 3.2.7 Pilot whale – explanatory model

This analysis included visual detections recorded as pilot whale; there were no acoustic detections of this species. This was the only species to be modelled as groups rather than individuals.

There were 8,313 modelled survey effort segments for pilot whale. Of these, 110 (1.04%) segments contained one or more sighting.

The best model included static covariates only and retained aspect, depth and distance to escarpments.

Table 11 and Figure 17 give the model results, including plots of the partial effect on density of the fitted smooth function for each model covariate. QQ and residuals plots are shown in Appendix 2. Figure 18 shows the distribution of density predicted from the model.

Density was predicted to be higher at depths greater than around 500m, at aspects between around 90° and 180° (towards the southeast), and to increase towards escarpments.

The geographical covariates X, Y were not retained in the predictive models for this species. Thus, the explanatory model serves as both predictive and explanatory models.

***Table 11. Results of the best explanatory model for pilot whales.***

| Error distribution | Model covariates | Estimated degrees of freedom | % Deviance explained | Model degrees of freedom |
|---|---|---|---|---|
| **Negative binomial** | Depth | 5.85 | 22.5 | 9.19 |
| | Distance to escarpments | 0.93 | | |
| | Aspect | 1.41 | | |

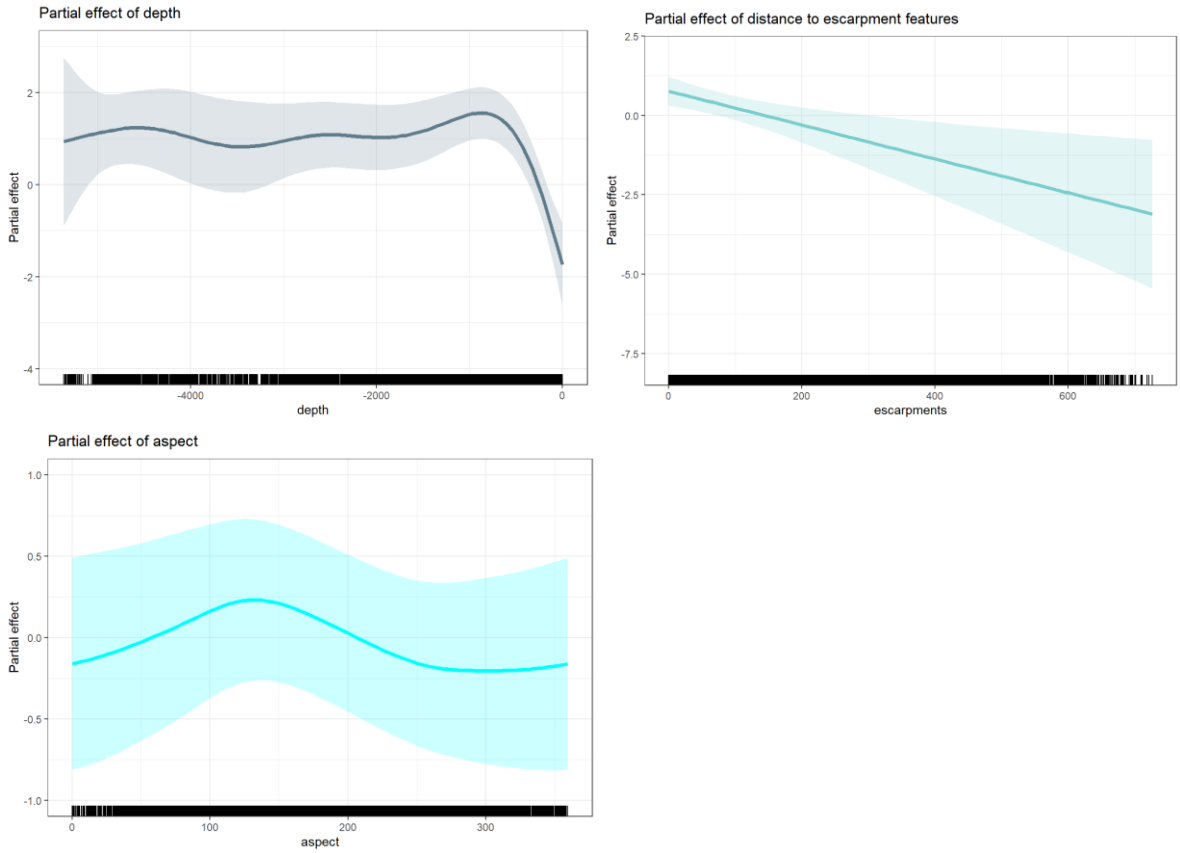


***Figure 17. Plots of the partial effect on density of covariates retained in the best explanatory model for pilot whales.***

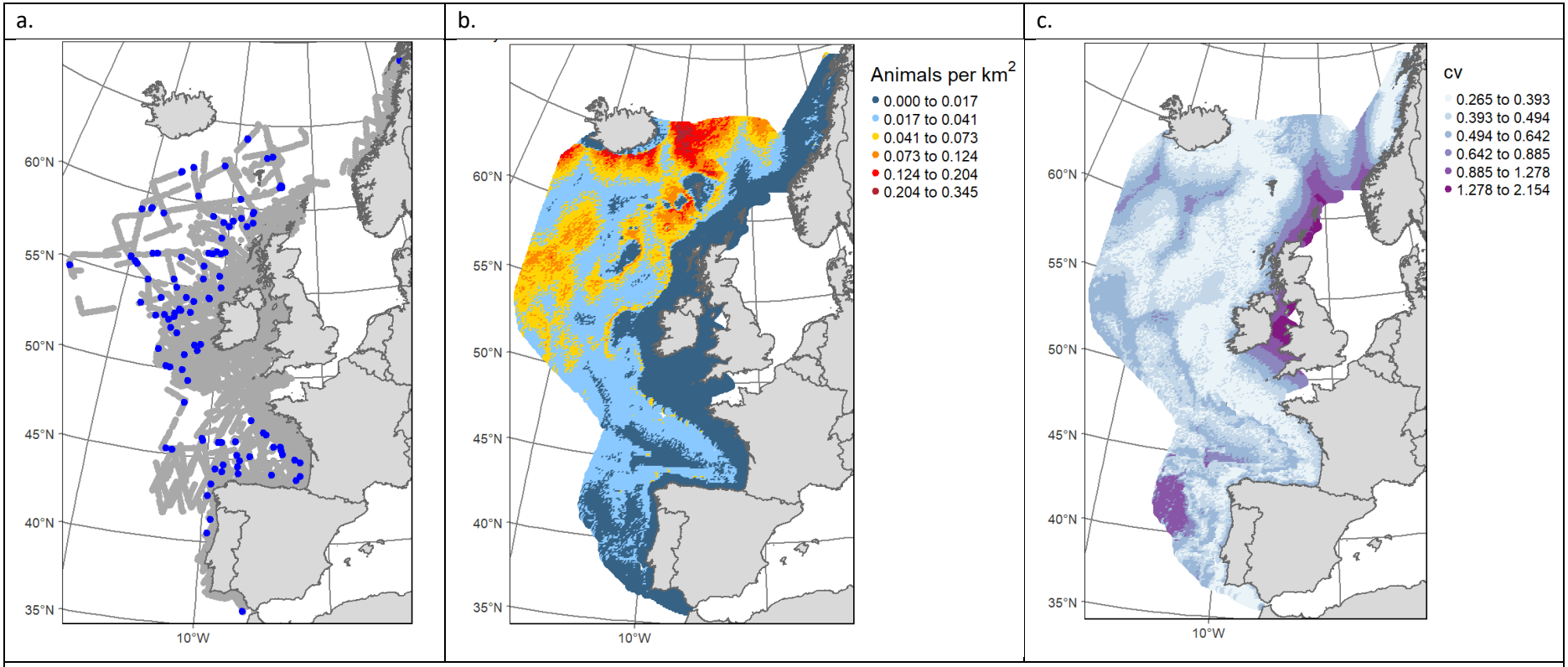


***Figure 18. (a) modelled effort and detections, (b) predicted density surface and (c) estimated CV surface for the best explanatory model for pilot whales.***

# 4 Discussion

## 4.1 Abundance estimates

The abundance estimates presented here for deep-diving cetaceans cover a large area of the European Atlantic, including all shelf waters and offshore waters out to 200nm from the coasts of the UK, Ireland, France and Spain. Offshore waters of Portugal are not included. As expected, the large proportion of abundance is estimated to be in offshore waters surveyed primarily by the NASS and SCANS-III ship surveys (Table 2).

The SCANS-III and NASS ship surveys used double-team methodology (Hammond et al. 2017; Pike et al. 2019) and all estimates presented here are corrected for perception bias (animals available to be detected but missed on the transect line where detection probability is assumed to be 1). The tracker survey mode employed on SCANS-III ships is designed also to correct for availability bias (animals present but unavailable to be detected on the transect line). However, the long dive times of deep diving species lead to a violation of the assumption that the probability of detection by the Primary team is independent of the probability of detection by the Tracker team because animals or groups seen by Tracker are likely to be underwater by the time that they become detectable by Primary. Therefore, the estimates of abundance of sperm, pilot and beaked whales from the SCANS-III ship surveys are only partially (at best) corrected for availability bias. Estimates from the SCANS-III and ObSERVE aerial surveys are not corrected either for perception or availability bias. Therefore, all estimates of abundance presented here are negatively biased to an unknown extent. However, the negative bias in estimates of pilot whale abundance is likely smaller than for sperm and beaked whales because pilot whale dive times are typically shorter and group sizes are considerably larger than for sperm and beaked whales (e.g., Cañadas et al. 2005; Heide-Jørgensen et al. 2002; Watwood et al. 2006).

The most abundant species of deep-diving cetacean in the area is the long-finned pilot whale, with the majority of animals (~50,000) and the highest density (~0.2 animals per $km^2$) estimated in the NASS survey area (Table 2). There were also an estimated ~20,000 animals (density ~0.05 animals per $km^2$) in offshore waters west of Scotland and in the Bay of Biscay. Results for the sperm whale followed a similar pattern of distribution but with smaller estimated abundance and density. There were ~20,000 animals (density ~0.08 animals per $km^2$) estimated in the NASS survey area and ~13,000 animals (density ~0.008 animals per $km^2$) estimated in offshore waters west of Scotland and in the Bay of Biscay (Table 2). The only beaked whale species with estimated overall abundance greater than 5,000 animals was the northern bottlenose whale, with ~14,000 animals (density ~0.05 animals per $km^2$) estimated in the NASS survey area (Table 2). However, the most abundant beaked whale within European waters was Cuvier's beaked whale with an estimated ~4,000 animals (density ~0.002 animals per $km^2$) in offshore waters west of Scotland and in the Bay of Biscay (Table 2).

All the estimates are rather imprecise, with CVs of abundance less than 0.4 only for sperm whale, pilot whale and Cuvier's beaked whale. The confidence intervals for most species are therefore wide. The primary reason for the lack of precision is that sample sizes are small.

### 4.1.1 Comparison with estimates from 2005-07

Table 3 compares estimates of sperm, pilot and beaked whales in 2015-16 with those from 2005-07 (Rogan et al. 2017). Estimates are for approximately the same survey area covered by NASS-15, SCANS-III and ObSERVE in 2015/16 and by SCANS-II, CODA and T-NASS-07 in 2005/07. The general pattern is that estimates were higher in 2005/07 than in 2015/16 for all species except the sperm whale, for which the estimate in 2015/16 is an order of magnitude greater than in 2005/07, and Cuvier's beaked whale, for which the estimates are very similar. Except for the sperm whale, the lack of precision in the estimates results in there being no statistically significant differences but the power to detect a difference if there were one is very low so inferences about differences in true abundance are inappropriate. The large difference in estimated abundance of sperm whale is unexplained.

## 4.2 Distribution

Beaked whales, as a group, are one of the least well known taxa on the planet, with a new species, Ramari's beaked whale (*Mesoplodon eueu*) being described in 2021 (Carroll et al. 2021), and the first live sighting of a species (Sato's beaked whale – *Berardius minimus*), which had previously only been known through stranding records, occurring in 2021 (Fedutin et al. 2022). The lack of understanding about distribution and abundance is problematic because there is an increasing requirement for such information to improve management and mitigation. For example, there is growing acceptance that beaked whale strandings are frequently associated with loud anthropogenic sounds (e.g. Jepson et al. 2003; D'Amico et al. 2009).

With field data on these taxa being so difficult to collect, approaches such as that employed here, in which multiple surveys are combined to model the influence of habitat features and to produce a density surface, have the potential to be very useful, as long as the resultant predictions are accurate representations of the species being modelled. Rogan et al. (2017) previously combined SCANS-II, CODA and T-NASS data to produce predicted density surfaces for the species modelled in this report. This study builds on this work, by modelling the most recently available visual survey data and also incorporating detections from passive acoustic monitoring. Rogan et al. (2018) found all modelled species had distributions that were significantly related to depth, distance from the 2000m isobath, variability in the seabed (modelled in their study as contour index) and sea surface temperature.

When so little Is known about the study taxa, choice of covariates to model can be challenging. Claro et al. (2020) proposed the use of seafloor geomorphic features rather than proxy covariates (for example, modelling the location of canyons specifically, rather than depth contours). That approach has been integrated into the models presented here, with escarpment features (steep slopes separating two relatively level areas) commonly being retained in the model. As with Rogan et al. (2018), depth was retained in all models where it was included as a candidate covariate. Due to correlation with sea bottom temperature, if the latter covariate was retained (e.g., sperm whale) depth was not included. In almost all cases where the relevant covariates were retained, geomorphological features were selected in preference to proxy isobaths. This is in broad agreement with the work of Claro et al. (2020).

A total of 10 different covariates were retained across the models presented in this report. Of these, depth was the most frequently retained, in five out of seven models. For the remaining two models,

depth could not be included because it was correlated with sea bottom temperature which had been selected for these species as the better covariate to include (and was retained in both cases).

Distance to escarpment features was also frequently retained, in four models. Escarpment features are associated with transition areas to deeper water, and whilst the two were not found to be correlated, they are possibly indicating similar types of relationships with habitat and prey.

The following discussion of results from models for all species relates to the explanatory models.

### 4.2.1 All beaked whales

Due to limited numbers of detections, previous studies have often combined beaked whales into a single category and modelled their distribution together (e.g. Rogan et al. 2017; Virgili et al. 2019). As with all of the individual species models, the combined beaked whale model from this study predicted peak densities of beaked whales at depths of at least 1000m, but also increased density with proximity to escarpment features and a U-shaped relationship with sea surface temperature (SST) with the lowest density of beaked whales occurring in waters with an SST around 15°C. These results differ slightly from the models produced by Virgili et al. (2019), but their study contained many more data points, which may explain the differences. Other studies have shown evidence for niche separation in beaked whales; modelling all species together may obscure the relationships between species and their environment (Visser et al. 2022).

### 4.2.2 Sowerby's beaked whale

The field detections of Sowerby's beaked whale fall into two main areas; one to the north-west of Scotland and Ireland, the other along the southern edge of the Bay of Biscay (Fig 10a). The model predictions (Fig 10b) reflect this distribution but also predict higher densities along the continental shelf slope, particularly to the southwest of Ireland (south of Porcupine Bank), and also in deeper waters to the northwest of Spain (west of Galicia). Precision of the prediction is better where density is predicted to be higher but is overall poor (Fig 10c).

The best model for this species predicts that shallower mixed layer depths would have positive effects on density and that as the mixed layer deepens density is predicted to decrease. However, the confidence interval surrounding the fitted relationship is very wide, so caution is needed in interpreting this result.

Peak densities are predicted at a sea bottom temperature of around 6°C. However, the confidence interval around the fitted function becomes very wide as the temperature increases, likely due to a lack of data at these temperatures, again limiting any inference that can be made from this result.

Unlike other deep-diving species, Sowerby's beaked whales are thought to feed primarily on small mid-water fish, which generally occur at depths up to 750m (Pereira et al. 2011), with stomach samples from the northwest Atlantic reporting more than 30 taxa (Wenzel et al. 2013). Analysis of acoustic data of Sowerby's beaked whales has found dive profiles consistent with whales selectively foraging on energetic prey items, potentially targeting larger individuals within a prey community (Visser et al. 2022). Our results showing an association between density and shallower mixed layer depths suggest that Sowerby's beaked whales are generally found in a nutrient-rich environment, which would support the hypothesis of selection of larger, higher energy prey items. Barile et al. (2021)

published models of acoustic detections and environmental parameters, which show the influence of SST, SSH and chlorophyl A concentration on Sowerby's beaked whale. Even with the pooled data, our dataset was limited to a very low number of detections. It is likely that the increased number of detections in the Barile et al. (2021) study, which resulted from the static acoustic deployments, allowed for the retention of more predictors in the final model.

### 4.2.3 Northern bottlenose whale

Field detections of northern bottlenose whale were all made in the northern part of the study region (Fig 12a). The model predictions (Fig 12b) reflect this distribution but also predict higher densities in waters to the west and southwest of Spain and Portugal. Precision of the prediction is better where density is predicted to be higher but is overall poor (Fig 12c).

The final model retained no dynamic predictors, only aspect, depth and distance to fan features. The slope for aspect is very flat and has a very wide confidence interval throughout the range of values, precluding any inference from this result. Predicted density of northern bottlenose whale is highest in waters at least 1000m deep, and at around 500km or more from fan features. Since fan features are predominantly in the south of the region, far from the locations of the field detections for this species, it is possible that this covariate is acting as a proxy for latitude, and inferences concerning distribution should not be based on this relationship.

This species is primarily specialist at preying on squid, so the strong relationship with depth is not unexpected. There are telemetry records of this species regularly making dives in excess of 800m (Hooker and Baird 1999).

### 4.2.4 Cuvier's beaked whale

Cuvier's beaked whale sightings were loosely scattered throughout the study region, with a cluster in the southern Bay of Biscay (Fig 14a). The model predictions (Fig 14b) do not reflect this distribution well but instead predict the highest densities off the edge of the continental shelf slope, particularly to the west of Spain and Portugal. However, precision of predicted density is overall poor (Fig 14c). The best model for this species retained only depth, distance to escarpment features and SD depth. Predicted density of this species increases linearly with depth and proximity to escarpment features.

Cuvier's beaked whales are canonically deep divers (Shearer et al. 2019) and feed both day and night, deep in the water column. They have been recorded to prey on at least 47 different species, primarily squid (Baird 2018). Other studies have reported relationships with sea surface height and other indicators of eddies and upwelling (Correia et al. 2015; Barile et al. 2021), suggesting these are areas in which prey aggregate.

### 4.2.5 Sperm whale

Sperm whale sightings were distributed in deep waters all through the study region (Fig 16a). The model predictions (Fig 16b) reflect this, with the highest densities predicted along the shelf slope and particularly in offshore waters in the northern part of the region. However, precision of predicted density is overall poor (Fig 16c).

The best model for sperm whale retained sea bottom temperature (SBT), sea level anomaly, mixed layer depth and distance to escarpment features. Except for SBT, all of the fitted relationships have

very wide confidence intervals, requiring caution when interpreting these relationships. The retention of SBT in the final model is in agreement with Virgili et al. (2022), who found deep water variables to be much better predictors of sperm whale density than for beaked whales.

#### 4.2.6 Pilot whale

Pilot whale sightings were also distributed in deep waters all through the study region, but with an apparent hiatus west of the southern Bay of Biscay and northwest Spain (Fig 18a). The model predictions (Fig 18b) reflect this overall in the northern part of the region, but not in the Bay of Biscay, likely because encounter rates are lower in this area. Precision of predicted density is overall better than for other species, primarily because of larger sample size, and confidence in these results is thus greater (Fig 18c).

The pilot whale model shows peak predicted density of pilot whales in water depths greater than 1000m, and close to escarpment features. Aspect is also retained as a covariate, showing a slight preference for south-east facing slopes but the confidence interval around the fitted smooth function is wide. The diet of this species comprises mostly small cephalopods. Escarpment features increase upwelling in the water column, which increases productivity and aggregates prey species (Fiedler, 2018), which would explain the modelled relationships with these features.

### 4.3 Methodological considerations

#### 4.3.1 Sample size

The modelling undertaken in this report is limited by the small number of sightings for most species. Recognising this from the start, considerable effort was expended attempting to add additional data from the Seabirds at Sea Team, but it ultimately proved impossible to fit informative models because including these data resulted in a much smaller proportion of effort segments with detections. Similarly, seasonal modelling not possible with systematic survey data because of small sample size - almost no data were collected outwith summer.

#### 4.3.2 Modelling methods

The modelling in this paper was conducted using the number of individuals (or groups) as the response variable, accounting for variation in detection probability by including an offset in the models, where the offset was equal to the segment length multiplied by the effective strip half width, as estimated from prior distance sampling analysis and reported in Hammond et al. (2021), CODA (2009) and Rogan et al. (2018). This method allows the segment width to expand and contract with environmental conditions but is unable to accommodate variation in detection probability due to covariates that change at the sighting level (such as sighting cue or group size).

An alternative is to model $\widehat{N}$, the count of individuals (or groups) divided by detection probability, as the response variable, in which case the offset is simply the segment length multiplied by twice the truncation distance used to estimate detection probability. This method maintains a constant width of each segment and incorporates variation in detection probability at the sighting level, thus allowing sighting-related covariates to be included.

As discussed above, a limiting factor in modelling most of these deep diving species in the European Atlantic is the sample size available and the very strong overdispersion introduced in the data because

of this. One possibility could be to explore hurdle models, in which models of the probability of presence are fitted first, followed by models of density conditional on probability of presence.

Whether these alternative modelling approaches would lead to greater insights regarding deep diving cetacean distribution and habitat use is unclear, but it might be worth pursuing such methods.

### 4.3.3 Explanatory vs predictive modelling

Predictive models were only presented for all beaked whales combined because the XY 2-D smooth function was not retained when included as a candidate in the single species models (but see Sowerby's beaked whale below). In terms of model performance, for all beaked whales combined the explanatory model explained less deviance in the data than the predictive model (28.7% vs 35.9%). This is to be expected because the XY 2-D smooth function in the predictive model is able to explain purely spatial variation in the data. These values are comparable with other cetacean modelling studies (e.g. Becker et al. 2017; Gilles et al. 2016; Virgili et al. 2019).

As described above, for Sowerby's beaked whale, the XY 2-D smooth function was retained in the predictive model, along with the covariates depth, SD depth and distance to the 1000m depth contour but a useable prediction could not be generated. This is likely because of over-fitting of the model.

#### *4.3.3.1 Covariates retained by the two models for all beaked whales combined*

For all beaked whales combined, the explanatory model retained the covariates depth, distance to escarpment features and sea surface temperature. The predictive model retained XY, and also depth and sea surface height. The only covariate retained by both models was depth. The fitted relationship between density and depth was very similar for both models (Figure 19), which suggests that this relationship is reflective of an important ecological process for this group of species. The rapid increase in predicted density as depth reaches 1000m is expected for deep diving species.

The lack of other shared covariates could be a result of several different factors. This model was fitted to data spanning a large latitudinal range from multiple species, which may have different habitat requirements. Variables other than depth, such as sea surface temperature, may not be useful predictors for multi-species models with a range of habitat preferences, even though these species are similar morphologically and physiologically.

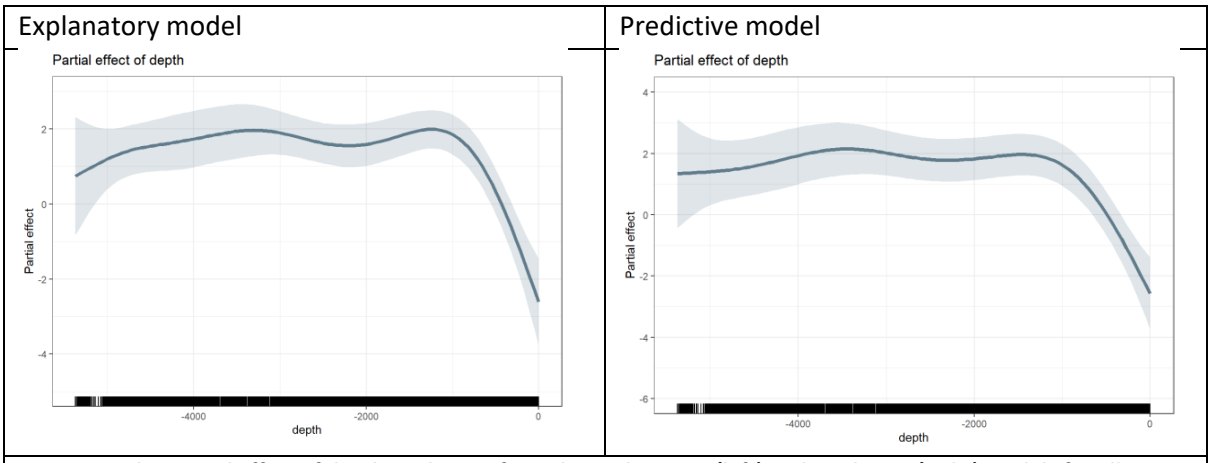


***Figure 19. The partial effect of depth on density from the explanatory (left) and predictive (right) models for all beaked whales combined, showing the very similar relationships for the two models.***

#### 4.3.3.2 *Predicted distributions from the models for all beaked whales combined*

The distributions of all beaked whales combined predicted by explanatory and predictive models are shown in Figure 20. Comparing the two, the explanatory model predicts much larger areas of medium density, including into areas with no field detections. The predictive model more closely matches the field detections, with areas of high predicted density focussed into more localised patches. The reason for this difference is that the XY 2-D smooth function included in the predictive model explains purely spatial variation in the data. This element is absent from the explanatory model, the prediction from which is a function only of the fitted relationships between density and environmental covariates. Both models predict areas of high density between northern Britain and Iceland, and in the southern part of the Bay of Biscay.

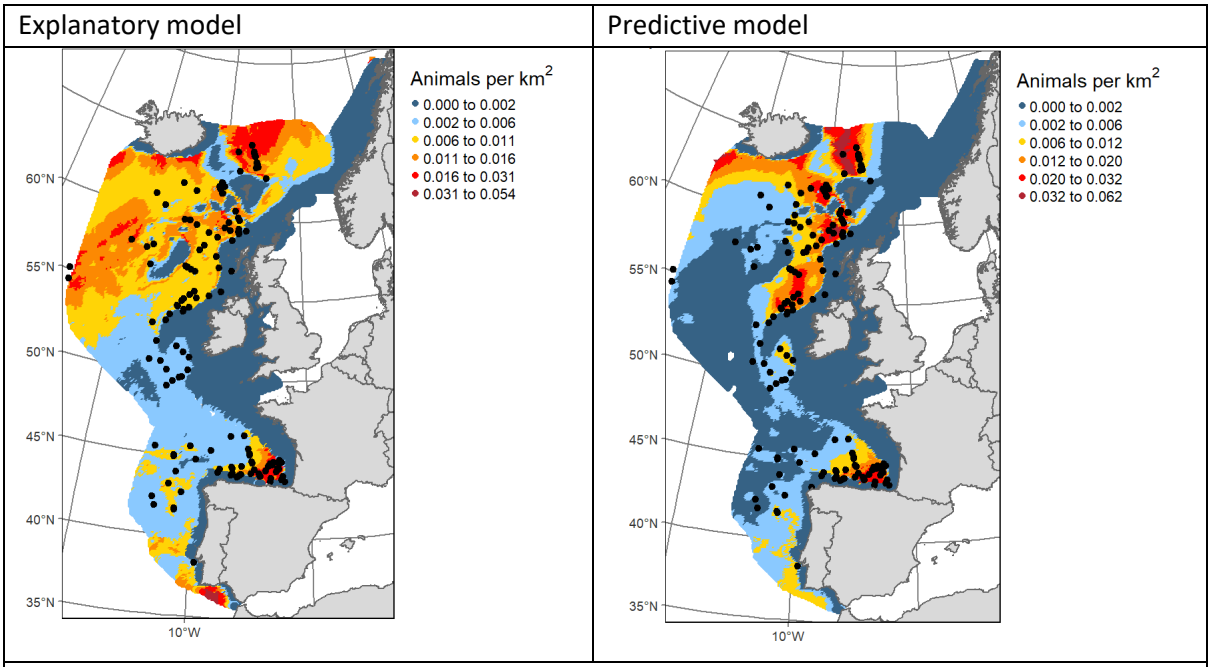


***Figure 20. Predicted density of all beaked whales combined for the explanatory (left) and predictive (right) models. Detections are overlaid on the predictions as black dots.***

### 4.3.4 Concluding remarks

Ultimately, investigating habitat relationships and distribution of deep diving species remains challenging, both because of the difficulty in obtaining data that can be modelled, and because the species of interest are most likely to be responding to environmental features at depth, for which there is a lack of covariate data. Nevertheless, our results are in broad agreement with previous studies, showing that the use of seafloor covariates such as escarpment features improves the models (Claro et al. 2020), and also that static features may be of more value in predicting beaked whale habitat, while dynamic features are more useful for sperm whales (Virgili et al. 2022). Although not used in this study, biological covariates such as minimum dissolved oxygen and hypoxic depth have been incorporated into models of beaked whales in the California Current Ecosystem, and have been found not to improve the predictions for beaked whale species, although this approach was more successful for sperm whales (Fiedler et al. 2023).

# 5 References


Aguilar de Soto, N., Madsen, P.T., Tyack, P., Arranz, P., Marrero, J., Fais, A., Revelli, E., and Johnson, M. 2012. No shallow talk: Cryptic strategy in the vocal communication of Blainville's beaked whales. Mar. Mammal Sci. **28**(2): E75–E92. doi:10.1111/j.1748-7692.2011.00495.x.

Amante, C., and Eakins, B.W. 2009. ETOPO1 1 Arc-Minute Global Relief Model: Procedures, Data sources and analysis. NOAA Technical Memorandum NESDIS NGDC-24.

Aoki, K., Sato, K., Isojunno, S., Narazaki, T., and Miller, P.J.O. 2017. High diving metabolic rate indicated by high-speed transit to depth in negatively buoyant long-finned pilot whales. J. Exp. Biol. **220**(20): 3802–3811. doi:10.1242/jeb.158287.

Baird, R., Borsani, J., Hanson, M., and Tyack, P. 2002. Diving and night-time behavior of long-finned pilot whales in the Ligurian Sea. Mar. Ecol. Prog. Ser. **237**: 301–305. doi:10.3354/meps237301.

Baird, R.W. 2018. Cuvier's Beaked Whale. *In* Encyclopedia of Marine Mammals. Elsevier. pp. 234–237. doi:10.1016/B978-0-12-804327-1.00100-X.

Barile, C., Berrow, S., and O'Brien, J. 2021. Oceanographic Drivers of Cuvier's (*Ziphius cavirostris*) and Sowerby's (*Mesoplodon bidens*) Beaked Whales Acoustic Occurrence along the Irish Shelf Edge. J. Mar. Sci. Eng. **9**(10): 1081. doi:10.3390/jmse9101081.

Barlow, J. 1999. Trackline detection probability for long-diving whales. *In* Marine Mammal Survey and Assessment Methods, edited by G. W. Garner, S. C. Amstrup, J. L. Laake, B. F. J. Manly, L. L. McDonald, and D. G. Robertson A.A. Balkema, Rotterdam. pp. 209–224.

Barlow, J., Ferguson, M.C., Perrin, W.F., Ballance, L., Gerrodette, T., Joyce, G., Mullin, K., Palka, D.L., and Waring, G. 2006. Abundance and densities of beaked and bottlenose whales (family *Ziphiidae*). J. Cetacean Res. Manage. **7**(3): 263-270.

Baumann-Pickering, S., McDonald, M.A., Simonis, A.E., Solsona Berga, A., Merkens, K.P.B., Oleson, E.M., Roch, M.A., Wiggins, S.M., Rankin, S., Yack, T.M., and Hildebrand, J.A. 2013. Species-specific beaked whale echolocation signals. J. Acoust. Soc. Am. **134**(3): 2293–2301. doi:10.1121/1.4817832.

Becker, E., Forney, K., Fiedler, P., Barlow, J., Chivers, S., Edwards, C., Moore, A., and Redfern, J. 2016. Moving Towards Dynamic Ocean Management: How Well Do Modeled Ocean Products Predict Species Distributions? Remote Sens. **8**(2): 149. doi:10.3390/rs8020149.

Becker, E.A., Forney, K.A., Thayre, B.J., Debich, A.J., Campbell, G.S., Whitaker, K., Douglas, A.B., Gilles, A., Hoopes, R., and Hildebrand, J.A. 2017. Habitat-Based Density Models for Three Cetacean Species off Southern California Illustrate Pronounced Seasonal Differences. Front. Mar. Sci. **4**: 121. doi:10.3389/fmars.2017.00121.

Breen, P., Pirotta, E., Allcock, L., Bennison, A., Boisseau, O., Bouch, P., Hearty, A., Jessopp, M., Kavanagh, A., Taite, M., and Rogan, E. 2020. Insights into the habitat of deep diving odontocetes around a canyon system in the northeast Atlantic ocean from a short multidisciplinary survey. Deep-Sea Res. Part I **159**: 103236. doi:10.1016/j.dsr.2020.103236.

Candy, S.G. 2004. Modeling catch and effort data using Generalised Linear Models, the Tweedie Distriution, Random Vessel Effects and Random Stratum-by-Year effects. CCAMLR Sci. **11**: 59–80.

Carroll, E.L., McGowen, M.R., McCarthy, M.L., Marx, F.G., Aguilar, N., Dalebout, M.L., Dreyer, S., Gaggiotti, O.E., Hansen, S.S., van Helden, A., Onoufriou, A.B., Baird, R.W., Baker, C.S., Berrow, S., Cholewiak, D., Claridge, D., Constantine, R., Davison, N.J., Eira, C., Fordyce, R.E., Gatesy, J., Hofmeyr, G.J.G., Martín, V., Mead, J.G., Mignucci-Giannoni, A.A., Morin, P.A., Reyes, C., Rogan, E., Rosso, M., Silva, M.A., Springer, M.S., Steel, D., and Olsen, M.T. 2021. Speciation in the deep: genomics and morphology reveal a new species of beaked whale *Mesoplodon eueu*. Proc. R. Soc. B Biol. Sci. **288**(1961): 20211213. doi:10.1098/rspb.2021.1213.

Casey, K.S., Brandon, T.B., Cornillon, P., and Evand, R. 2010. The Past, Present and Future of the AVHRR Pathfinder SST Program. *In* Oceanography from Space. Springer.

Claro, B., Pérez-Jorge, S., and Frey, S. 2020. Seafloor geomorphic features as an alternative approach into modelling the distribution of cetaceans. Ecol. Inform. **58**: 101092. doi:10.1016/j.ecoinf.2020.101092.

CODA. 2009. Cetacean Offshore Distribution and Abundance in the European Atlantic (CODA). Final Report. University of St Andrews, UK. Available from https://archive.st-andrews.ac.uk/biology/coda/.

Correia, A.M., Tepsich, P., Rosso, M., Caldeira, R., and Sousa-Pinto, I. 2015. Cetacean occurrence and spatial distribution: Habitat modelling for offshore waters in the Portuguese EEZ (NE Atlantic). J. Mar. Syst. **143**: 73–85. doi:10.1016/j.jmarsys.2014.10.016.

D'Amico, A., Gisiner, R.C., Ketten, D.R., Hammock, J.A., Johnson, C., Tyack, P.L., and Mead, J. 2009. Beaked Whale Strandings and Naval Exercises. Aquat. Mamm. **35**(4): 452–472. doi:10.1578/AM.35.4.2009.452.

Fedutin, I.D., Filatova, O.A., Meschersky, I.G., and Hoyt, E. 2022. First confirmed observations of living Sato's beaked whales *Berardius minimus*. Mar. Mammal Sci. **38**:1676–1681. doi:10.1111/mms.12936.

Fernandez, E., and Lellouche, J.M. 2021. Product User Manual: For the Global Ocean Physical Reanalysis product Global_Reanalysis_Phy_001_030.

Fiedler, P.C. 2018. Ocean Environments. *In* Encyclopedia of Marine Mammals, 3rd edition. Elsevier. pp. 649–653.

Fiedler, P.C., Becker, E.A., Forney, K.A., Barlow, J., and Moore, J.E. 2023. Species distribution modeling of deep-diving cetaceans. Mar. Mammal Sci. **39**: 1178-1203. doi:10.1111/mms.13057.

Gilles, A., Viquerat, S., Becker, E.A., Forney, K.A., Geelhoed, S.C.V., Haelters, J., Nabe-Nielsen, J., Scheidat, M., Siebert, U., Sveegaard, S., Beest, F.M., Bemmelen, R., and Aarts, G. 2016. Seasonal habitat-based density models for a marine top predator, the harbor porpoise, in a dynamic environment. Ecosphere **7**(6). doi:10.1002/ecs2.1367.

Hammond, P., Lacey, C., Gilles, A., Viquerat, S., Börjesson, P., Herr, H., Macleod, K., Ridoux, V., Santos, M., Teilmann, J., Vingada, J., and Øien, N. 2021. Estimates of cetacean abundance in European Atlantic waters in summer 2016 from the SCANS-III aerial and shipboard surveys. https://scans3.wp.st-andrews.ac.uk/files/2021/06/SCANS-III_design-based_estimates_final_report_revised_June_2021.pdf

Hammond, P.S., Macleod, K., Berggren, P., Borchers, D.L., Burt, L., Cañadas, A., Desportes, G., Donovan, G.P., Gilles, A., Gillespie, D., Gordon, J., Hiby, L., Kuklik, I., Leaper, R., Lehnert, K., Leopold, M., Lovell, P., Øien, N., Paxton, C.G.M., Ridoux, V., Rogan, E., Samarra, F., Scheidat, M., Sequeira, M., Siebert, U., Skov, H., Swift, R., Tasker, M.L., Teilmann, J., Van Canneyt, O., and Vázquez, J.A. 2013. Cetacean abundance and distribution in European Atlantic shelf waters to inform conservation and management. Biol. Conserv. **164**: 107–122. doi:10.1016/j.biocon.2013.04.010.

Harris, P.T., Macmillan-Lawler, M., Rupp, J., and Baker, E.K. 2014. Geomorphology of the oceans. Mar. Geol. **352**: 4–24. doi:10.1016/j.margeo.2014.01.011.

Heide-Jørgensen, M.P., Bloch, D., Stefansson, E., Mikkelsen, B., Ofstad, L.H., and Dietz, R. 2002. Diving behaviour of long-finned pilot whales Globicephala melas around the Faroe Islands. Wildl. Biol. **8**(4): 307–313.

Hooker, S.K., and Baird, R.W. 1999. Deep-diving behaviour of the northern bottlenose whale, Hyperoodon ampullatus (Cetacea: Ziphiidae). Proc. R. Soc. B Biol. Sci. **266**(1420): 671. doi:10.1098/rspb.1999.0688.

Jain, G.C., and Consul, P.C. 1971. A Generalized Negative Binomial Distribution. SIAM J. Appl. Math. **21**(4): 501–513. Society for Industrial and Applied Mathematics. doi:10.1137/0121056.

Jaquet, N., Dawson, S., and Slooten, E. 2000. Seasonal distribution and diving behaviour of male sperm whales off Kaikoura: foraging implications. Can. J. Zool. **78**: 13.

Jepson, P.D., Arbelo, M., Deaville, R., Patterson, I.A.P., Castro, P., Baker, J.R., Degollada, E., Ross, H.M., Herráez, P., Pocknell, A.M., Rodríguez, F., Howie, F.E., Espinosa, A., Reid, R.J., Jaber, J.R., Martin, V., Cunningham, A.A., and Fernández, A. 2003. Gas-bubble lesions in stranded cetaceans. Nature **425**(6958): 575–576. doi:10.1038/425575a.

Johnson, M., Madsen, P.T., Zimmer, W.M.X., Aguilar de Soto, N., and Tyack, P.L. 2004. Beaked whales echolocate on prey. Proc. R. Soc. Lond. B Biol. Sci. **271**(suppl_6). doi:10.1098/rsbl.2004.0208.

Lambert, E., Pierce, G.J., Hall, K., Brereton, T., Dunn, T.E., Wall, D., Jepson, P.D., Deaville, R., and MacLeod, C.D. 2014. Cetacean range and climate in the eastern North Atlantic: future predictions and implications for conservation. Glob. Change Biol. **20**(6): 1782–1793. doi:10.1111/gcb.12560.

MacLeod, C.D. 2017. Beaked whales, overview. *In* Encyclopedia of Marine Mammals, Third Edit. *Edited by* B. Würsig, J.G.M. Thewissen, and K. Kovacs. Academic Press. pp. 80–83. doi:10.1016/B978-0-12-804327-1.00062-5.

Macleod, C.D., Perrin, W.F., Pitman, R., Barlow, J., Ballance, L., D'Amico, A., Gerrodette, T., Joyce, G., Mullin, K.D., Palka, D.L., and Waring, G.T. 2006. Known and inferred distributions of beaked whale species (Cetacea: Ziphiidae). J. Cetacean Res. Manage. **7**(3): 271–286. doi:10.47536/jcrm.v7i3.737.

Marra, G., and Wood, S.N. 2011. Practical variable selection for generalized additive models. Comput. Stat. Data Anal. **55**(7): 2372–2387. doi:10.1016/j.csda.2011.02.004.

McGeady, R., McMahon, B.J., and Berrow, S. 2016. The effects of seismic surveying and environmental variables on deep diving odontocete stranding rates along Ireland's coast. Proc. Meet. Acoust. **27**(1). doi:10.1121/2.0000281.

Miller, P.J.O., Johnson, M.P., Madsen, P.T., Biassoni, N., Quero, M., and Tyack, P.L. 2009. Using at-sea experiments to study the effects of airguns on the foraging behavior of sperm whales in the Gulf of Mexico. Deep-Sea Res. Part Oceanogr. Res. Pap. **56**(7): 1168–1181. Elsevier. doi:10.1016/j.dsr.2009.02.008.

Nowacek, D.P., Clark, C.W., Mann, D., Miller, P.J.O., Rosenbaum, H.C., Golden, J.S., Jasny, M., Kraska, J., and Southall, B.L. 2015. Marine seismic surveys and ocean noise: Time for coordinated and prudent planning. Front. Ecol. Environ. **13**(7): 378–386. doi:10.1890/130286.

Pante, E., and Simon-Bouhet, B. 2013. marmap: A package for importing, plotting and analyzing bathymetric and topographic data in r. PLoS ONE **8**(9): e73051.

Pereira, J.N., Neves, V.C., Prieto, R., Silva, M.A., Cascão, I., Oliveira, C., Cruz, M.J., Medeiros, J.V., Barreiros, J.P., Porteiro, F.M., and Clarke, D. 2011. Diet of mid-Atlantic Sowerby's beaked whales Mesoplondon bidens. Deep Sea Res. Part Oceanogr. Res. Pap. **58**(11): 1084–1090. doi:10.1016/j.dsr.2011.08.004.

Pike, D., Gunnlaugsson, T., Mikkelsen, B., Halldórsson, S.D., and Víkingsson, G. 2019. Estimates of the abundance of cetaceans in the central North Atlantic based on the NASS Icelandic and Faroese shipboard surveys conducted in 2015. NAMMCO Sci. Publ. **11**. doi:10.7557/3.4941.

Pike, D.G., Gunnlaugsson, T., Víkingsson, G.A., and Mikkelsen, B. 2008. Estimates of the abundance of fin whales (*Balaenoptera physalus*) from the T-NASS Icelandic and Faroese ship surveys conducted in 2007. Document SC/60/PFI13 presented to the IWC Scientific Committee.

Pitman, R. 2018. Mesoplodon Beaked Whales. *In* Encyclopedia of Marine Mammals, 3rd Edition. Elsevier. pp. 595–602. doi:10.1016/B978-0-12-804327-1.00172-2.

Rogan, E., Breen, P., Mackey, M., Cañadas, A., Scheidat, M., Geelhoed, S., and Jessopp, M. 2018. Aerial Surveys of Cetaceans and Seabirds in Irish waters: Occurrence, distribution and abundance in 2015-2017. Department of Communications, Climate Action & Environment and National Parks and Wildlife Service (NPWS), Department of Culture, Heritage and the Gaeltacht, Dublin, Ireland. 297pp.

Rogan, E., Cañadas, A., Macleod, K., Santos, M.B., Mikkelsen, B., Uriarte, A., Van Canneyt, O., Vázquez, J.A., and Hammond, P.S. 2017. Distribution, abundance and habitat use of deep

diving cetaceans in the North-East Atlantic. Deep-Sea Res. Part II Top. Stud. Oceanogr. **141**(April): 8–19. Elsevier Ltd. doi:10.1016/j.dsr2.2017.03.015.

Shearer, J.M., Quick, N.J., Cioffi, W.R., Baird, R.W., Webster, D.L., Foley, H.J., Swaim, Z.T., Waples, D.M., Bell, J.T., and Read, A.J. 2019. Diving behaviour of Cuvier's beaked whales ( *Ziphius cavirostris* ) off Cape Hatteras, North Carolina. R. Soc. Open Sci. **6**(2): 181728. doi:10.1098/rsos.181728.

Stanistreet, J.E., Nowacek, D.P., Baumann-Pickering, S., Bell, J.T., Cholewiak, D.M., Hildebrand, J.A., Hodge, L.E.W., Moors-Murphy, H.B., Van Parijs, S.M., and Read, A.J. 2017. Using passive acoustic monitoring to document the distribution of beaked whale species in the western North Atlantic Ocean. Can. J. Fish. Aquat. Sci. **74**(12): 2098–2109. doi:10.1139/cjfas-2016-0503.

Stanistreet, J.E., Beslin W.A.M., Kowarski K., Martin B.S., Westell A., and Moors-Murphy H.B. 2022. Changes in the acoustic activity of beaked whales and sperm whales recorded during a naval training exercise off eastern Canada. Scientific Reports 12:1973 https://doi.org/10.1038/s41598-022-05930-4.

Tyack, P.L., Johnson, M., Soto, N.A., Sturlese, A., and Madsen, P.T. 2006. Extreme diving of beaked whales. J. Exp. Biol. **209**(21): 4238–4253. doi:10.1242/jeb.02505.

Virgili, A., Authier, M., Boisseau, O., Cañadas, A., Claridge, D., Cole, T., Corkeron, P., Dorémus, G., David, L., Di-Méglio, N., Dunn, C., Dunn, T.E., García-Barón, I., Laran, S., Lauriano, G., Lewis, M., Louzao, M., Mannocci, L., Martínez-Cedeira, J., Palka, D., Panigada, S., Pettex, E., Roberts, J.J., Ruiz, L., Saavedra, C., Santos, M.B., Van Canneyt, O., Vázquez Bonales, J.A., Monestiez, P., and Ridoux, V. 2019a. Combining multiple visual surveys to model the habitat of deep-diving cetaceans at the basin scale: Large-scale modelling of deep-diving cetacean habitats. Glob. Ecol. Biogeogr. **28**(3): 300–314. doi:10.1111/geb.12850.

Virgili, A., Authier, M., Boisseau, O., Cañadas, A., Claridge, D., Cole, T.V.N., Peter Corkeron, Dorémus, G., David, L., Di-Méglio, N., Dunn, C., Dunn, T.E., García-Barón, I., Laran, S., Lauriano, G., Lewis, M., Louzao, M., Mannocci, L., Martínez-Cedeira, J., Palka, D.L., Panigada, S., Pettex, E., Roberts, J.J., Ruiz, L., Saavedra, C., Santos, M.B., Van Canneyt, O., Bonales, J.A.V., Monestiez, P., and Ridoux, V. 2019b. Combining multiple visual surveys to model the habitat of deep-diving cetaceans at the basin scale. Large-scale modelling of deep-diving cetacean habitats. Glob. Ecol. Biogeogr. **28**: 300–314. doi:DOI: 10.1111/geb.12850.

Virgili, A., Teillard, V., Dorémus, G., Dunn, T.E., Laran, S., Lewis, M., Louzao, M., Martínez-Cedeira, J., Pettex, E., Ruiz, L., Saavedra, C., Santos, M.B., Canneyt, O., Bonales, J.A.V., and Ridoux, V. 2022. Deep ocean drivers better explain sperm whales *Physeter macrocephalus* than beaked whale habitat preferences in the Bay of Biscay. Sci. Rep. **12**(1). https://doi.org/10.1038/s41598-022-13546-x.

Visser, F., Oudejans, M.G., Keller, O.A., Madsen, P.T., and Johnson, M. 2022. Sowerby's beaked whale biosonar and movement strategy indicate deep-sea foraging niche differentiation in mesoplodont whales. J. Exp. Biol. **225**(9): jeb.243728. doi:10.1242/jeb.243728.

Watkins, W.A., Daher, M.A., Fristrup, K.M., Howald, T.J., and di Sciara, G.N. 1993. Sperm whales tagged with transponders and tracked underwater by sonar. Mar. Mammal Sci. **9**(1): 55–67. doi:10.1111/j.1748-7692.1993.tb00426.x.

Watwood, S.L., Miller, P.J.O., Johnson, M., Madsen, P.T., and Tyack, P.L. 2006. Deep-diving foraging behaviour of sperm whales (*Physeter macrocephalus*). J. Anim. Ecol. **75**: 814–825.

Wenzel, F.W., Polloni, P.T., Craddock, J.E., Gannon, D.P., Nicolas, J.R., Read, A.J., and Rosel, P.E. 2013. Food habits of Sowerby's beaked whales (*Mesoplodon bidens*) taken in the pelagic drift gillnet fishery of the western North Atlantic. Fish. Bull. **111**(4): 381-389. https://doi.org/10.7755/FB.111.4.7

Zimmer, W.M.X., Harwood, J., Tyack, P.L., Johnson, M.P., and Madsen, P.T. 2008. Passive acoustic detection of deep-diving beaked whales. J. Acoust. Soc. Am. **124**(5): 2823–2832. doi:10.1121/1.2988277.

# 6 Appendix 1 – Maps of covariates retained in models of deep diving species

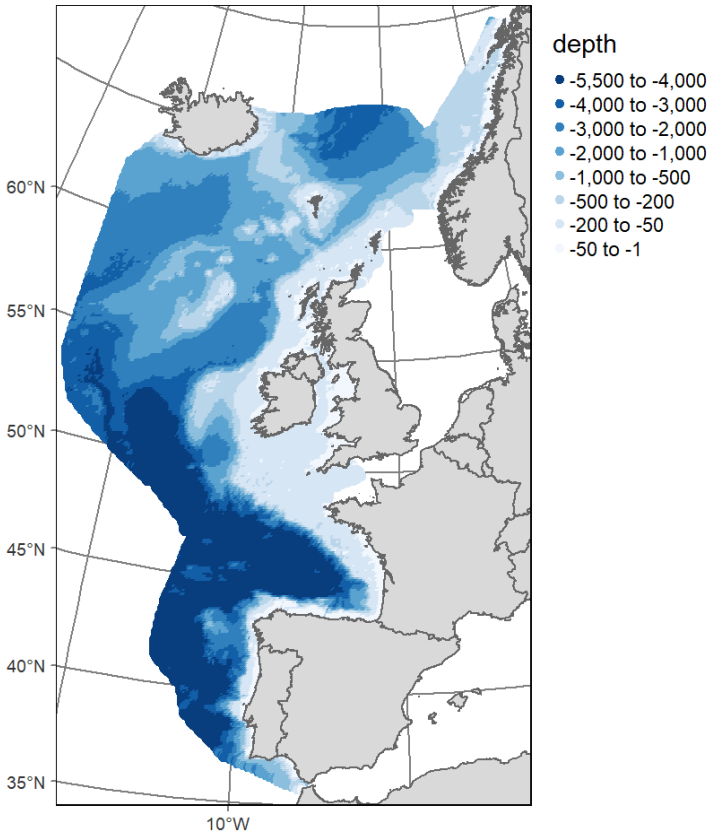


***A1. 1: Map showing water depth across the survey area***

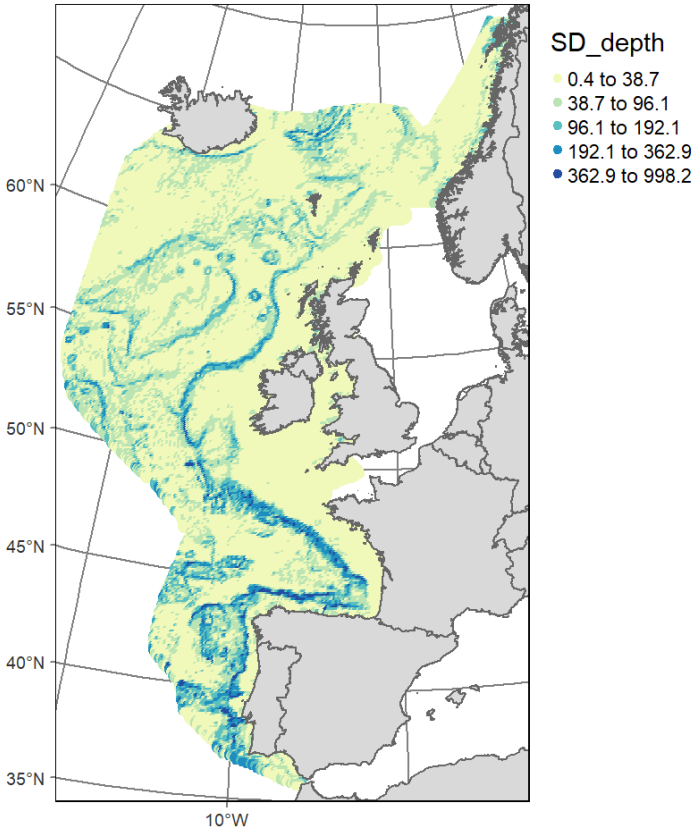


***A1. 2: Map showing standard deviation of water depth across the survey area***

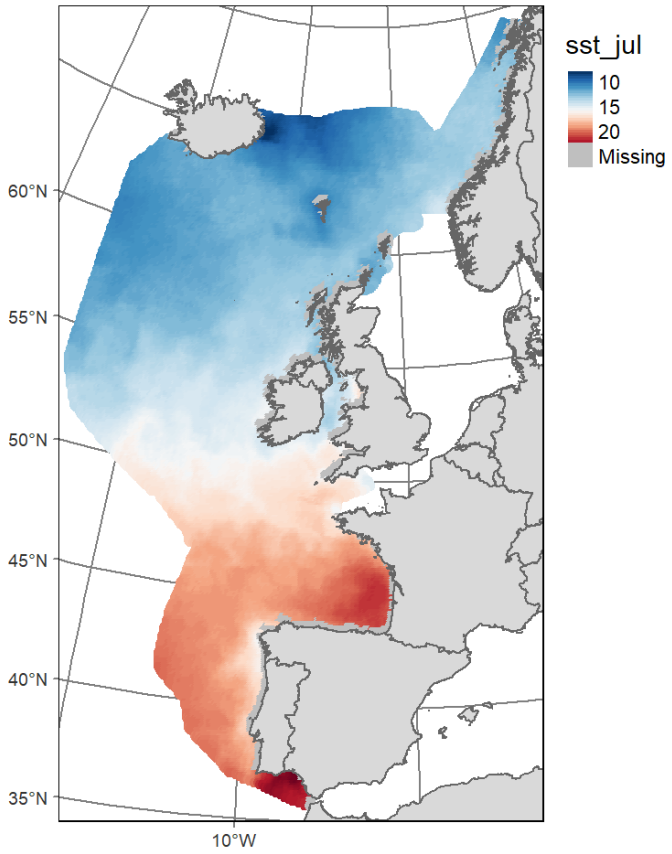


*A1. 3: Map showing mean sea surface temperature for July 2016 across the survey area*

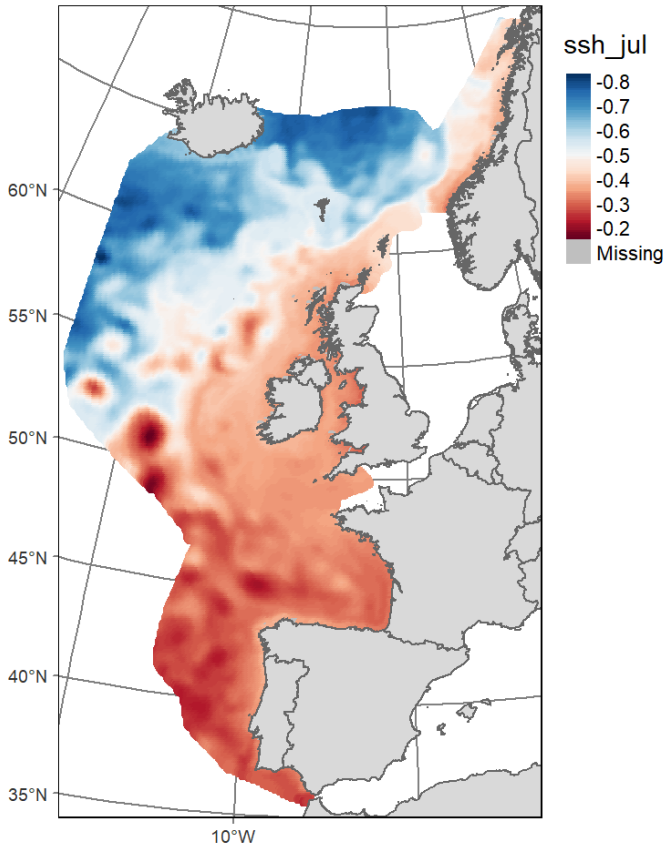


*A1. 4: Map showing mean sea surface height for July 2016 across the survey area*

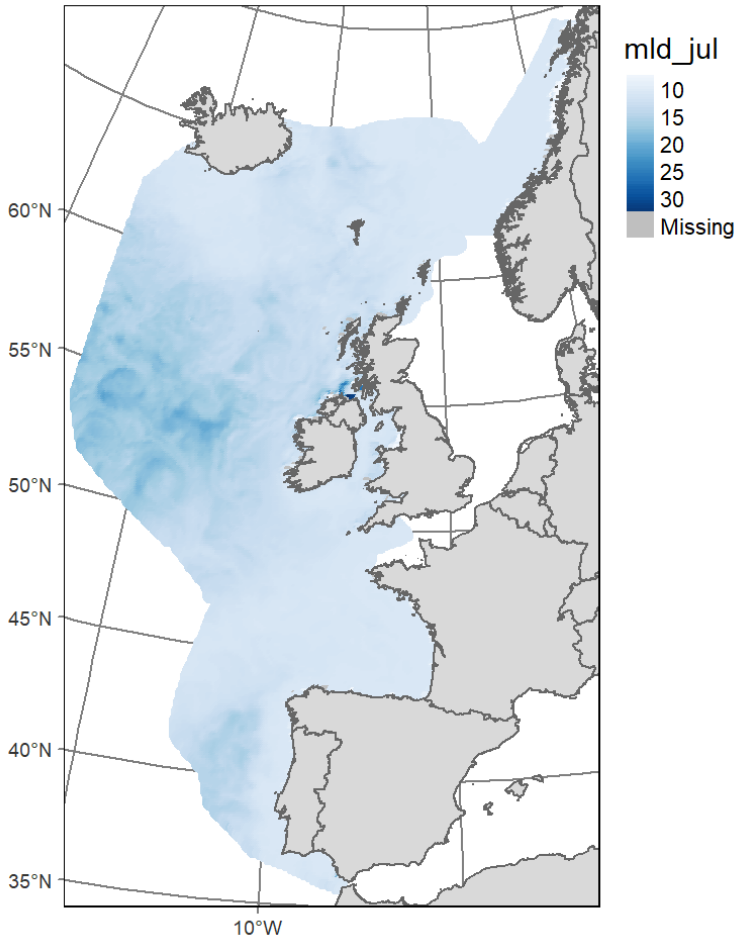


*A1. 5: Map showing mean mixed layer depth for July 2016 across the survey area*

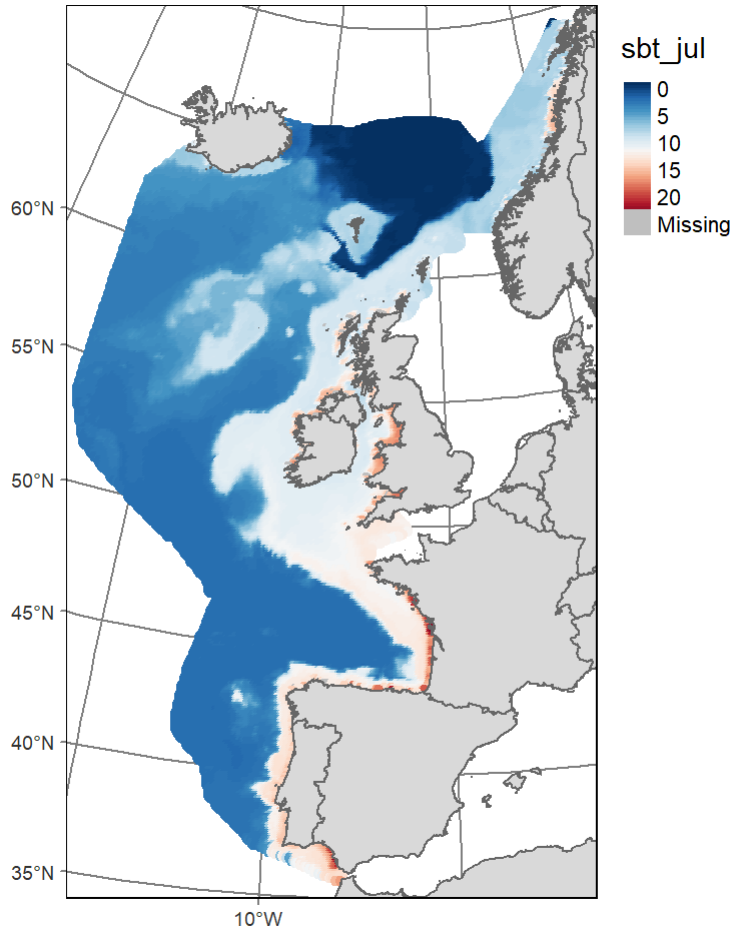


*A1.6: Map showing mean sea bottom temperature for July 2016 across the survey area*

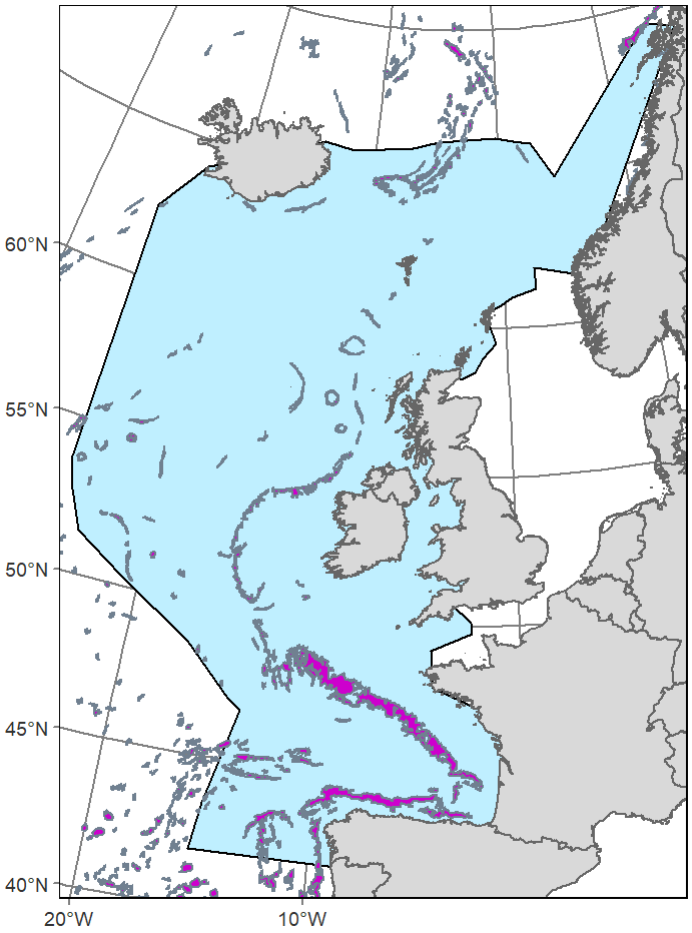


*A1. 7: Map showing the location of escarpment features (pink) across the study area (blue)*

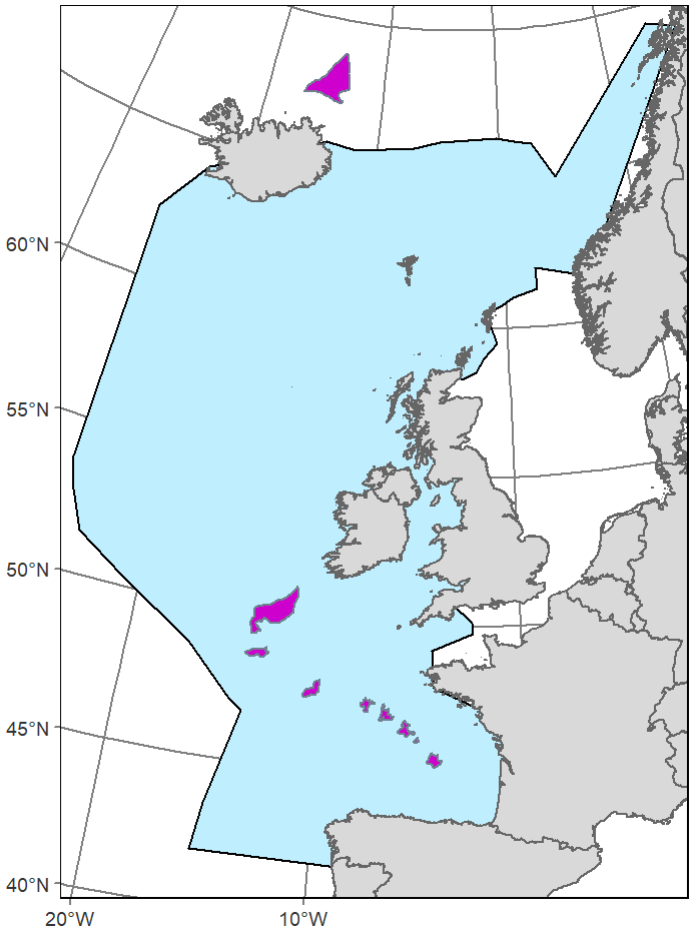


*A1.8: Map showing the location of fan features (pink) across the study area (blue)*

# 7 Appendix 2 – Residual and QQ plots for each of the species models

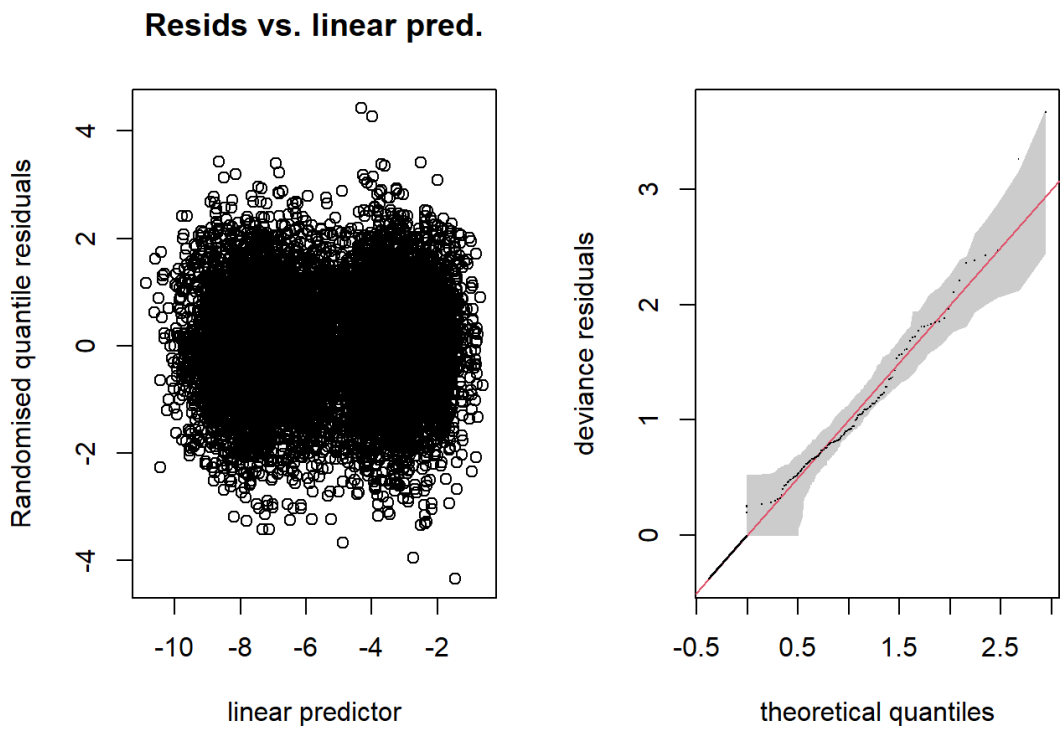


***A2. 1: Residual and QQ plots from the all beaked whales combined explanatory model***

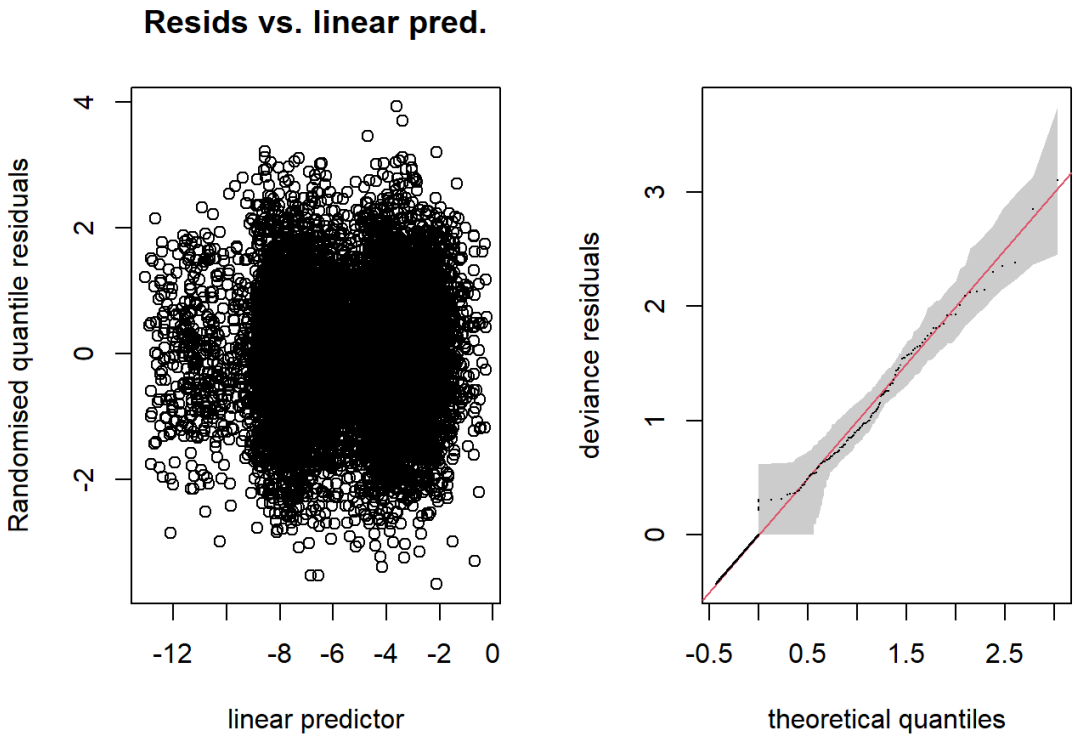


***A2. 2: Residual and QQ plots from the all beaked whales combined predictive model***

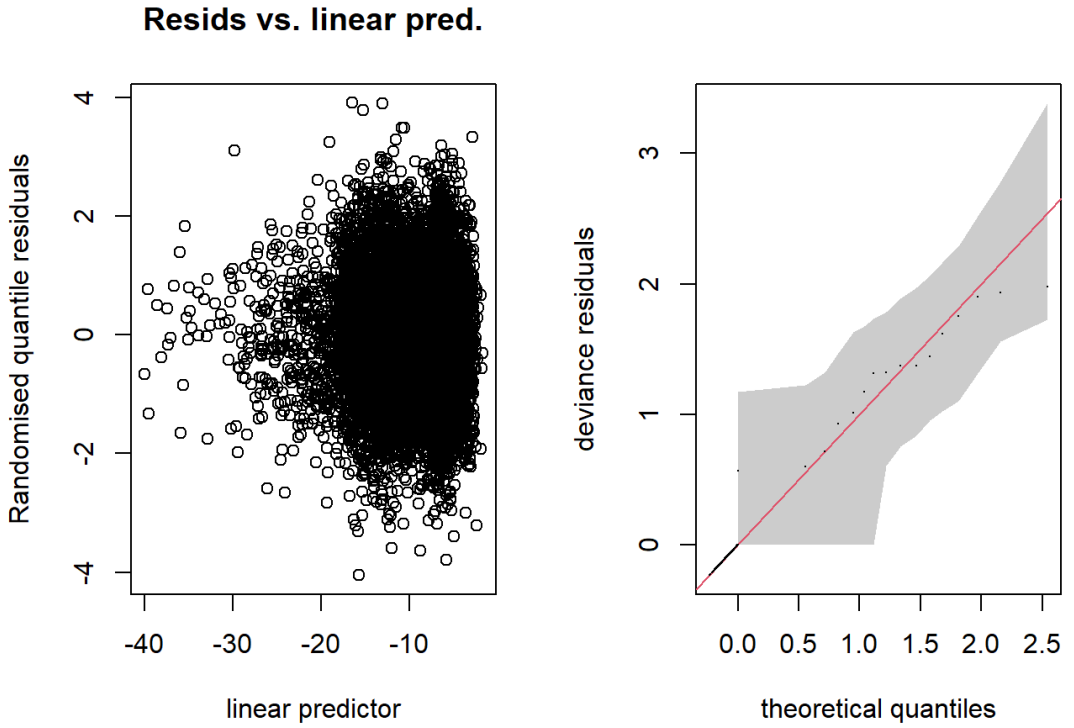


*A2. 3: Residual and QQ plots from the Sowerby's beaked whale explanatory model*

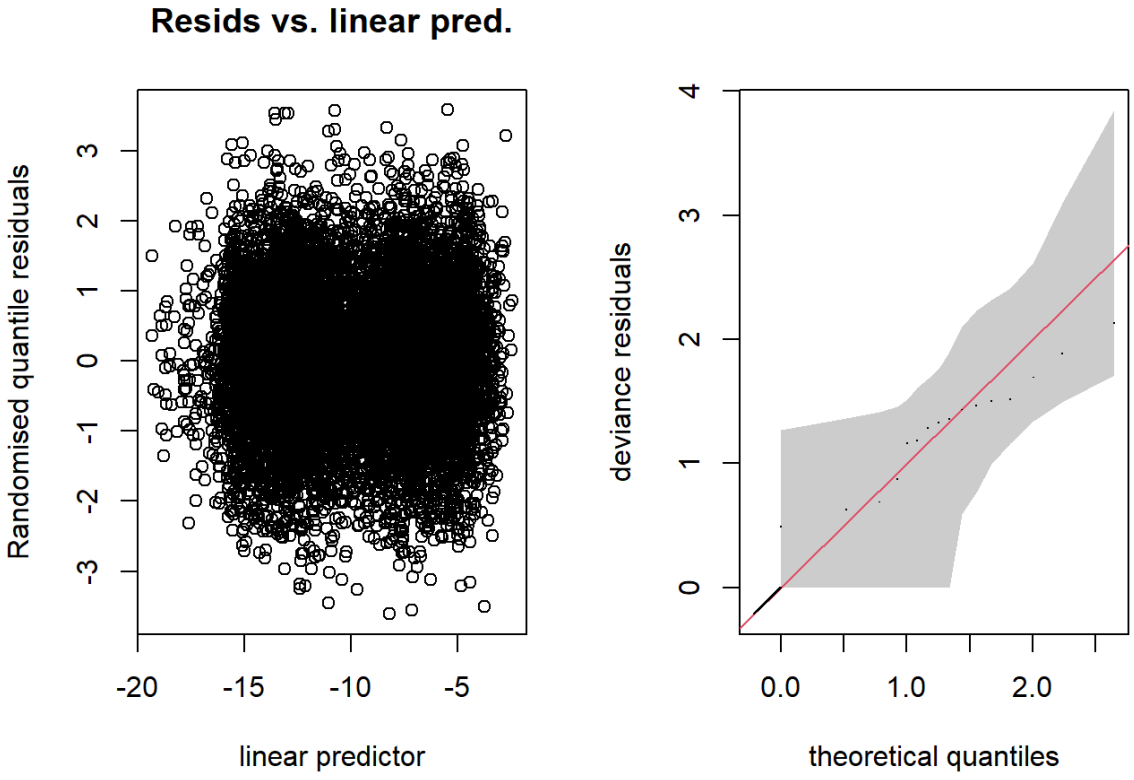


*A2. 4: Residual and QQ plots from the Sowerby's beaked whale predictive model*

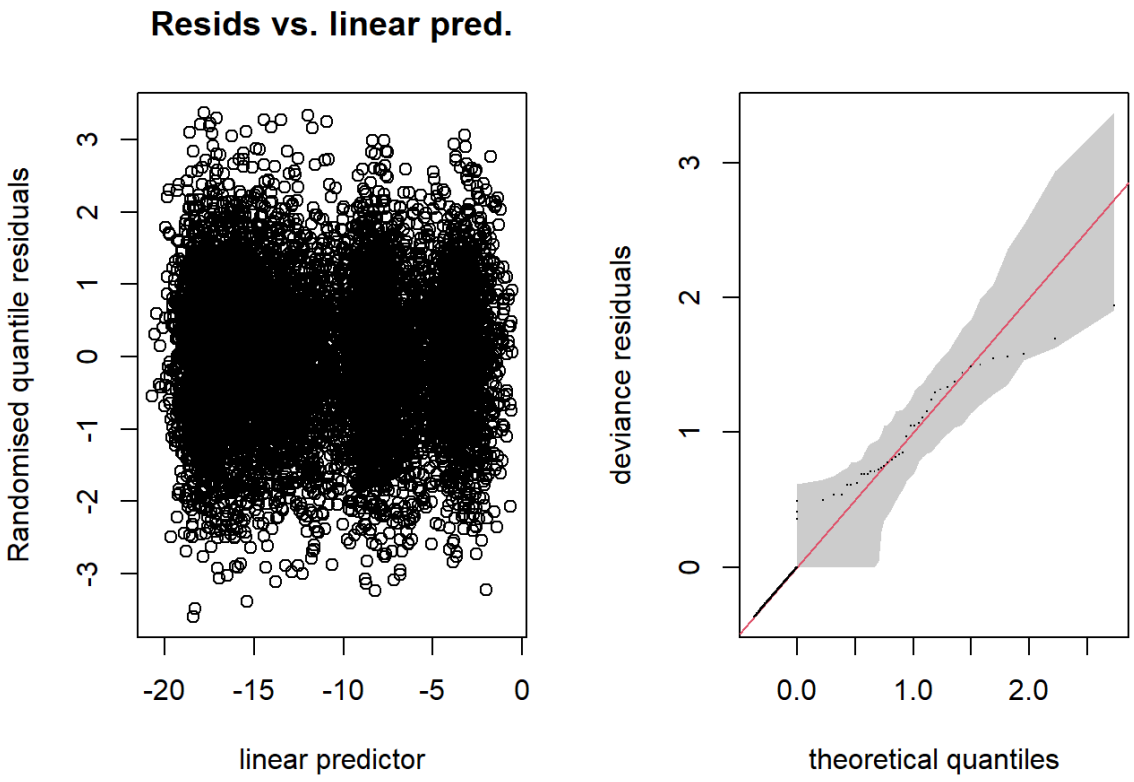


*A2. 5: Residual and QQ plots from the northern bottlenose whale explanatory model*

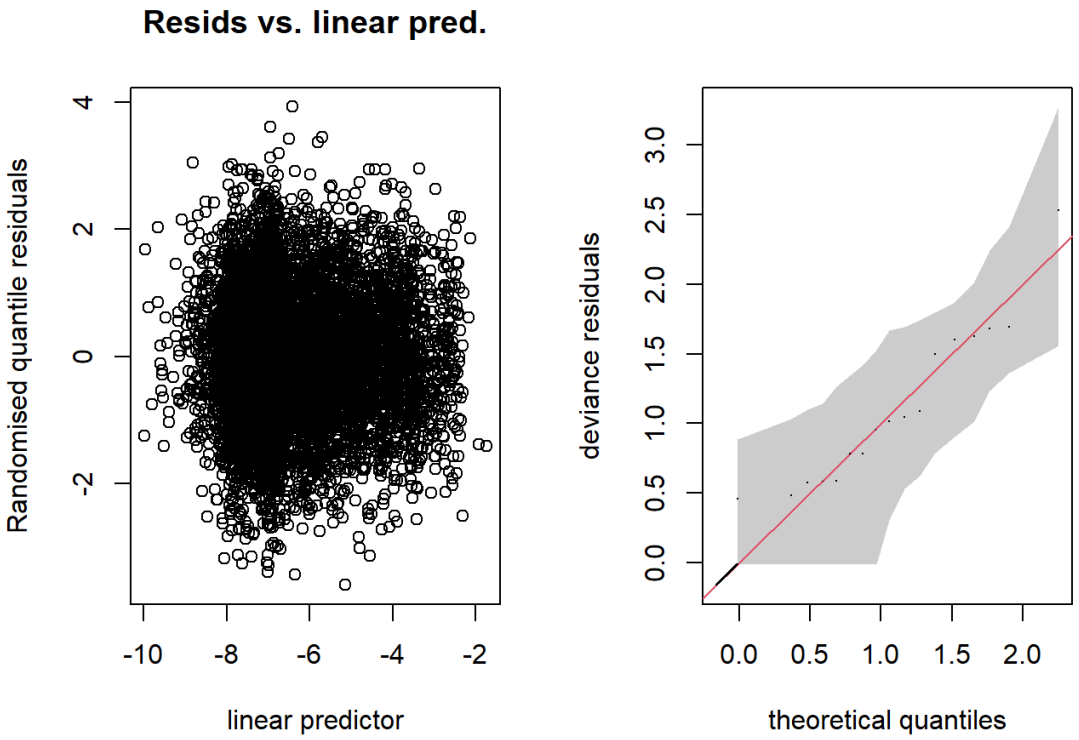


*A2. 6: Residual and QQ plots from the Cuvier's beaked whale explanatory model*

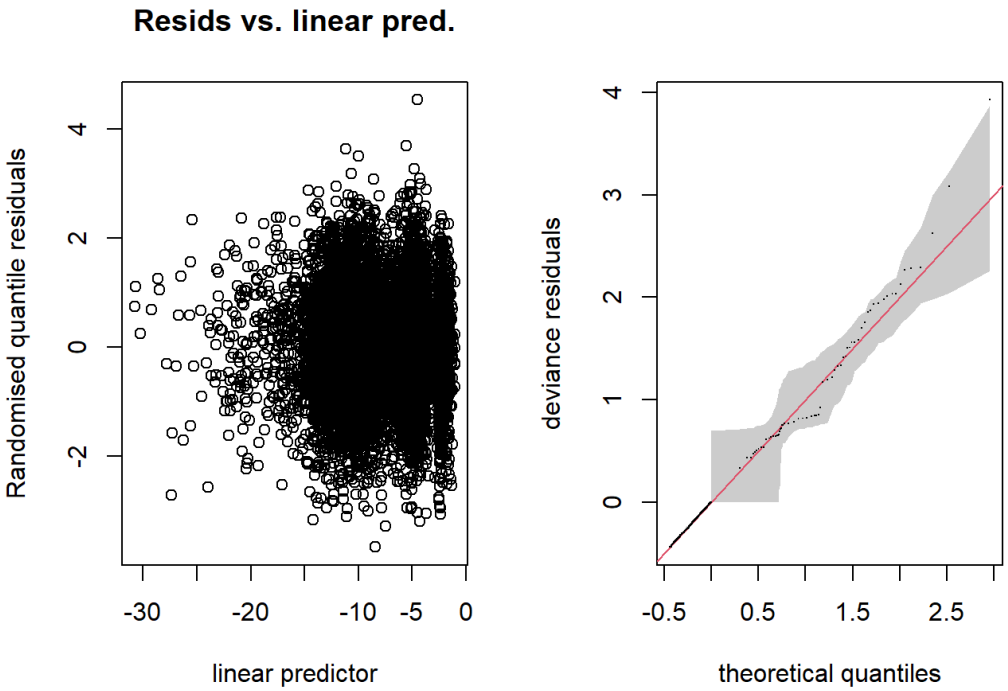


*A2. 7: Residual and QQ plots from the sperm whale explanatory model*

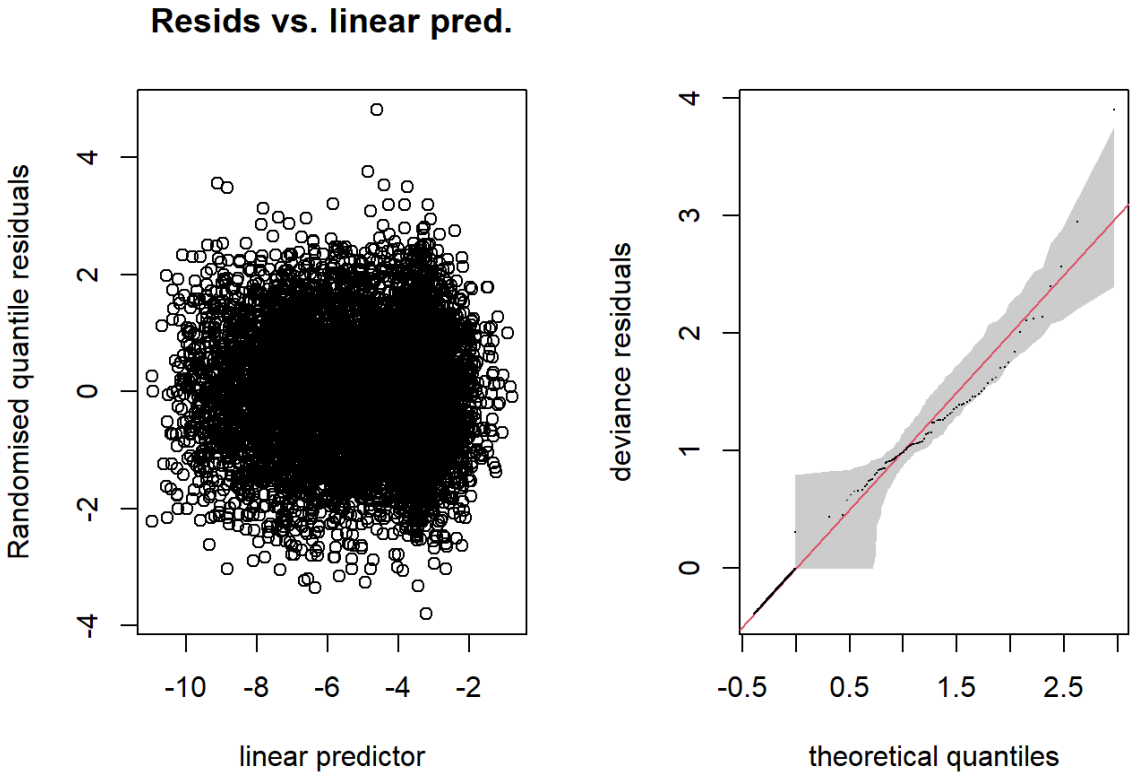


*A2. 8: Residual and QQ plots from the pilot whale explanatory model*